

Design for Reliability: Improving Reliability of Plastic Encapsulated Ocean Technology Products by Understanding Moisture Ingress through FEA Simulation

Junaid Shafaat

Consultant

St. John's, Newfoundland and Labrador, Canada

j.shafaat@gmail.com

Abstract

Remote sensing products designed for ocean environments sustain the harshness of cold oceans. The reliability of these telemetry devices needs to be very high to measure, collect and transmit data over a long period of time.

One of the biggest challenges for ocean technology products is moisture. Moisture poses a significant threat to the reliability of microelectronic assemblies, especially for scientific research products that are designed for marine environments and can be attributed as being one of the principal causes of many early-life failures. The presence of moisture in plastic packaging alters thermal stress through alteration of thermo-mechanical properties like, change of elastic modulus, shear strength and glass transition temperatures. Moisture also induces hygroscopic stress through differential swelling, reduces interfacial adhesion strength, induces corrosion and acts as an unwanted resistance when present between the two nodes of component and result in lowering the resistance which results in faster depletion of budgeted power.

In this study, failure modes in preliminary tests were analyzed through Weibull analysis. Design fault tree analysis made it easy to isolate the root cause of the early life failures, moisture intrusion. An analytical model was developed and validated both by experiments and simulation to determine the ingress rate of the moisture through the bi-material interface. After calculating diffusion coefficients of the two polyurethane materials, moisture ingress rate was calculated using an analytical model and also simulated through finite element analysis. Once the diffusivity coefficient is known, the theoretical Fickian curve is plotted with the experimental data to see if the absorption is Fickian or not. The 99% saturation approach helps to define the limit of Fickian diffusion hence eliminate error caused by non-fickian absorption. Since the diffusion coefficient is constant for a particular material, for bi-material analysis, interfacial concentration discontinuity cannot be analyzed as an interfacial discontinuity result where two materials having different saturated concentrations are joined. The results of ingress rate through FEA simulation came close to the calculated values hence validating the model.

Based on results and understanding of ingress rates through different materials and considering deployment designed life of product, proper selection of materials is made possible thus increasing the reliability of the product which is evident in plotted comparison survival graphs.

1. Introduction

Biotelemetry (or Medical Telemetry) involves the application of telemetry in the medical field to remotely monitor various vital signs of ambulatory patients. Telemetry is a technology that allows the remote measurement and reporting of information of interest to the system designer or operator, typically referring to wireless communication. Biotelemetry devices designed for marine life study varies in size and technology based upon environment and size of the animal, for example these tags can be equipped with multiple sensors like;

- Temperature sensors (environment and body temperature measurements)
- Pressure sensors (elevation for in-land and depth sensing for water animals)
- Motion sensors (mobility)
- Compass (to determine heading or positioning)
- Light Sensors (to determine day and night)



Figure 1 Data Recorders, courtesy of Lotek Wireless Inc.

Biotelemetry devices, especially data recorder tags as shown in Figure 1, are designed to study animal behaviors by tagging animals either externally on the body or internally (implanted) that monitor and record data over the mission of the study. This important data is usually recovered after a long wait by scientists and single tag can carry up to 32,000 data points which depict the behavior of the animal over a period of 3-4 years. The recovery rate of these tags is very low, in the range of 3.9-10%, (Walker and Urawa, 2007)[1], which makes it very important for these devices to have high system reliability so that during the mission, tags record data reliably and after the mission data can be obtained reliably from the recovered tags. Therefore, due to the risks involved, these data recording tags needs to have high reliability. Figure 2 shows some main components of the data recorder tag.

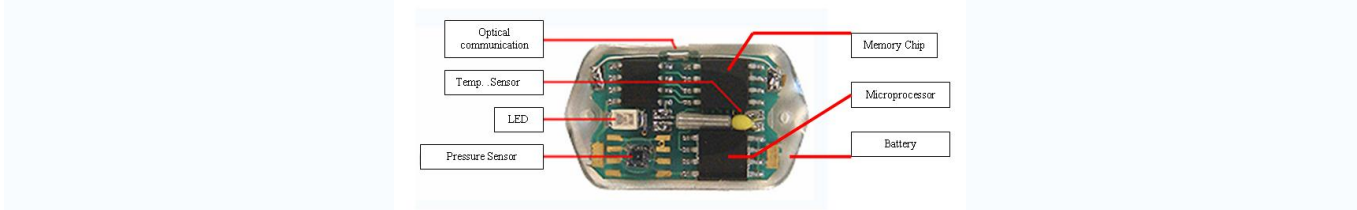


Figure 2 – Components of Data Recorder Tracking Tag, courtesy of Lotek Wireless Inc.

The product under study was failing prematurely during its mission phase and this paper is based on the study of data-recorder devices as shown in figure 2. The study starts with failure data analysis, identifying major failure modes and then further investigation of these failure modes to determine the root cause of the premature failures. The top two failure modes; Power and Packaging were investigated but this paper is focused mainly on packaging failures.

2. Failure Data Analysis

The hazard rate plotting method is used to determine the probability distribution that best describes the failure process. Hazard rate is defined by Equations (1) and (2);

$$\lambda(t) = \frac{f(t)}{R(t)} \tag{1}$$

$$\lambda(t) = \frac{f(t)}{1 - F(t)} \tag{2}$$

Where;

$\lambda(t)$ = hazard rate or instantaneous failure rate

$R(t)$ = reliability at time t

$f(t)$ = probability density function (PDF)

$F(t)$ = cumulative distribution function (CDF)

Weibull distribution consists of a family of distributions which can be used to describe a wide range of failure data. The Weibull density function is defined by Equation (3);

$$R(t) = e^{-\left(\frac{t}{\theta}\right)^\beta} \tag{3}$$

For $t \geq 0$

Where;

R = reliability of system at given time, t

t = time

β = shape parameter

θ = scale parameter (characteristic life)

The Exponential and the Raleigh distributions are two of the many special distributions that can be obtained from the Weibull distributions by changing the value of the shape parameter, β . An Exponential distribution is obtained by setting the shape

parameter to 1, while a Raleigh distribution is obtained by setting the shape parameter to 2. The failure and reliability functions are related by Equation (4);

$$F(t) = 1 - e^{-\left(\frac{t}{\theta}\right)^\beta} \tag{4}$$

Rearranging and applying natural log twice on both sides;

$$\ln \ln \left\{ \frac{1}{1 - F(t)} \right\} = \beta \ln t - \beta \ln \theta \tag{5}$$

Comparing equation (5) with the general equation (6), describing a straight line,

$$Y = mx + c \tag{6}$$

Where,

$$Y = \ln \ln \left\{ \frac{1}{1 - F(t)} \right\}$$

$$X = \ln t$$

A graph is plotted between $\ln \ln [1/(1-F(t))]$ and $\ln(t)$ using full failure data irrespective of failure modes, as shown below in Figure 3.

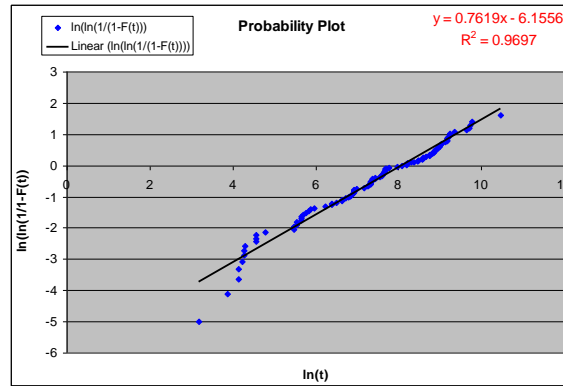


Figure 3 - Weibull Plot of Full Data (regardless of failure mode)

Considering equation (5) and comparing with the equation of the straight line, equation (6), from graph in figure 5, we can see that;

$$\text{Slope} = m = \beta = 0.7619$$

$0 < \beta < 1 = 0.76 =$ exponentially decreasing function, describes infant mortality

$$\theta = e^{-\frac{y}{\beta}} \tag{7}$$

$$\Theta = 3225.89 \text{ hours}$$

Similarly, MTTF for Weibull distribution can be calculated using Equation (8);

$$MTTF = \theta \cdot \Gamma \left(1 + \frac{1}{\beta} \right) \tag{8}$$

Inserting the values of θ and β from the graph and determining the value of Γ from the tables, we get;

MTTF = 3786.45 hours, or 0.43 years

We can see that the distribution is showing decaying hazard rate, $\lambda(t)$, which is the infant mortality part of the bathtub curve as shown in Figure 4 below.

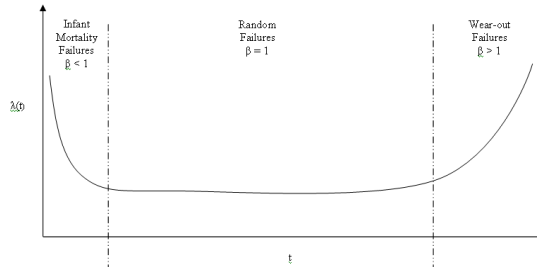


Figure 4 – Bathtub Curve

After analyzing the complete failure data broken down into different failure modes, the Pareto chart in Figure 5 shows all failure modes and their contribution.

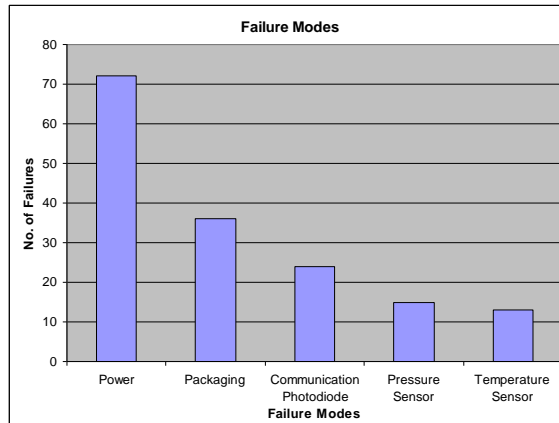


Figure 5 – Failure Modes Pareto Chart

Weibull analysis of each failure mode is also separately done as shown in figures 6-10, as shown below;

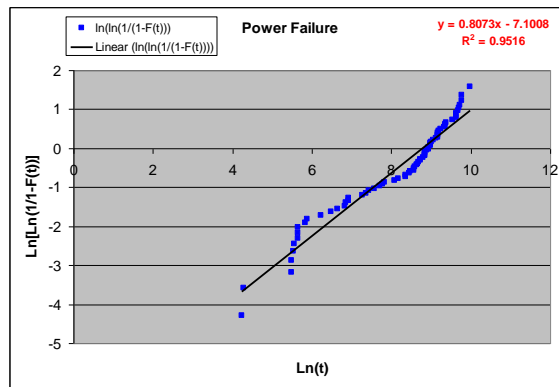


Figure 6 – Weibull Plot of Power Failure Data

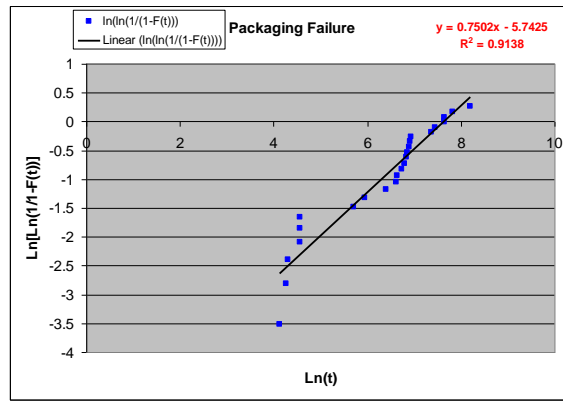


Figure 7 – Weibull Plot of Packaging Failure Data

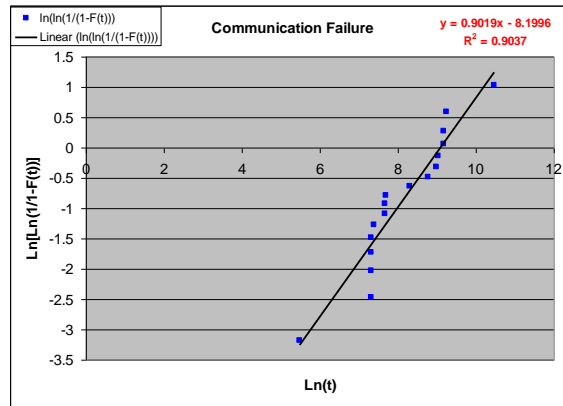


Figure 8 – Weibull Plot of Communications Failure Data

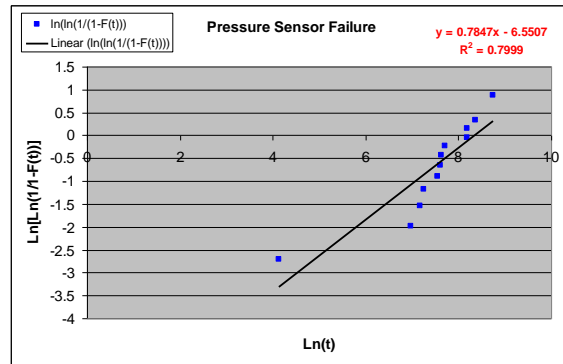


Figure 9 – Weibull Plot of Pressure Sensor Failure Data

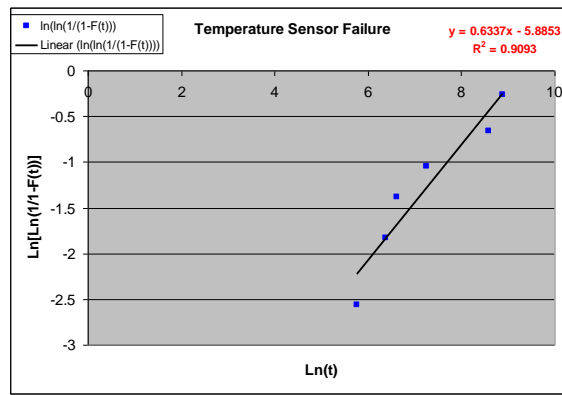


Figure 10 – Weibull Plot of Temperature Failure Data

A summary of the results from the Weibull plots is shown in Table 1;

Table 1 – Summary of Weibull Plots

Data Set	Shape Parameter	Scale Parameter	Result
All failures combined	$\beta = 0.76$	$\theta = 3225$	Infant Mortality
Power failure	$\beta = 0.80$	$\theta = 6606$	Infant Mortality
Packaging failure	$\beta = 0.75$	$\theta = 2110$	Infant Mortality
Communication failure	$\beta = 0.90$	$\theta = 8879$	Infant Mortality
Pressure failure	$\beta = 0.78$	$\theta = 4221$	Infant Mortality
Temperature failure	$\beta = 0.63$	$\theta = 10793$	Infant Mortality

These results show that the magnitude of the shape factor for the individual failure modes, as well as for the complete set of data is less than unity. This indicates that the tags failed in the “Infant Mortality” mode. This means that a better quality control system may actually reduce the failure rate of these tags and increase their service life. Reasons for failure in the different modes need to be explored in detail and manufacturing and assembly defects need to be eliminated before the deployment of these tags.

3. Fault Tree Analysis

A Fault Tree analysis was conducted to further investigate the root cause of these failures. Each mode of failure is plotted to show root cause of the failure and the probability of each component failure is looked upon to determine the root-cause of the failure. A block diagram of the whole system is constructed to show the relationship between components related to particular circuits which will help in creating and understanding the fault tree diagrams. Figure 11 shows the block diagram of the data recorder that is under study;

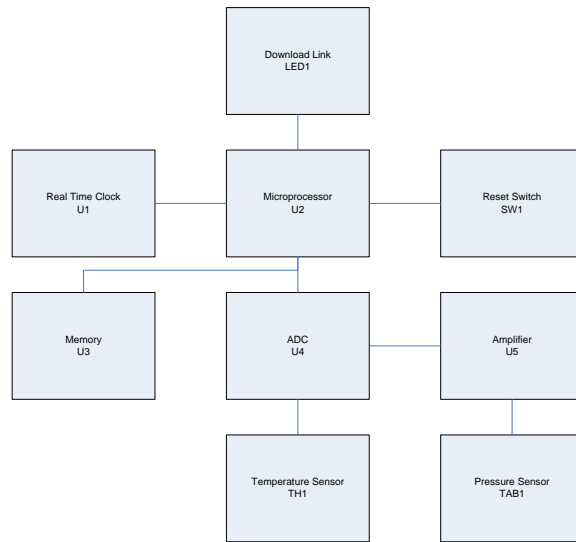


Figure 11 – Block Diagram of Data Recorder Tag

The DC power is supplied to the microprocessor (U2) which runs the embedded firmware to control the rest of the circuitry. Using MIL-HDBK-217F [2], failure rates of each component was calculated and corresponding failure probability values were determined for Fault Tree Analysis. The values are shown in the following Table 2;

Table 2 - Failure Rates of Components

Description	Reference Designator	Failure Rate/10 ⁶ hours	Quantity Used	Total Failure Rate/10 ⁶ hours	R(t) = exp(-λt)	F(t) = 1-R(t)
Diode KA3020SRC	LED1	0.011664	1	0.011664	0.999693517	0.000306483
Crystal Tuning Fork 32.768Hz	X1	0.12432	1	0.12432	0.996738202	0.003261798
RTC PCF8563TS	U1	0.0416	1	0.0416	0.998907349	0.001092651
MICRO PIC12LC509A-04I/SN	U2	0.208	1	0.208	0.994548673	0.005451327
EPROM 24LC515-I/SM	U3	2.02	1	2.02	0.948298835	0.051701165
CONV MCP3202-CI/ST	U4	0.0372	1	0.0372	0.999022862	0.000977138
AMP LMV358MM	U5	0.1256	1	0.1256	0.996704674	0.003295326
Trans UN9214	Q1	1.75E-03	1	0.00175	0.999954011	4.59889E-05
CAP CER 1.0uF 16V 0603	C1	2.31E-03	1	0.00231	0.999939295	6.0705E-05
CAP CER 22pF NPO 0603 5% 50V	C2	0.013	1	0.013	0.999658418	0.000341582
CAP CER 220pF NPO 0603 5% 50V	C3	0.024	1	0.024	0.999369479	0.000630521

CAP CER 1000pF X7R 0603 10% 50	C4	0.029	1	0.029	0.99923817	0.00076183
CAP CER 1.0uF 16V 0603	C5	2.98E-03	1	0.00298	0.999921689	7.83113E-05
CAP CER 0.01uF X7R 0603 10%50V	C6	1.79E-03	1	0.00179	0.99995296	4.70401E-05
CAP Tantalum 220uF 6V C- Case	C7	0.078	1	0.078	0.997952259	0.002047741
Resistor 100Kohm 1% 0603	R3,R9,R10,R11, R13	8.62E-03	5	0.0431	0.999773492	0.000226508
Resistor 10Kohm 1% 0603	R2,R8,R15	7.84E-03	3	0.02352	0.999793986	0.000206014
Resistor 15Kohm 1% 0603	R5	7.84E-03	1	0.00784	0.999793986	0.000206014
Resistor 43Kohm 5% 0603	R7	7.84E-03	1	0.00784	0.999793986	0.000206014
Resistor 18K2ohm 1% 0603	R14	7.84E-03	1	0.00784	0.999793986	0.000206014
Resistor 15Mohm 5% 0603	R6	0.0196	1	0.0196	0.999485045	0.000514955
Resistor 0ohm 5% 0603	R18	7.84E-03	1	0.00784	0.999793986	0.000206014
Sensor NTC Thermistor	TH1	0.441	1	0.441	0.988477419	0.011522581
PCB LTD1100 Version 2	PCB	0.0323	1	0.0323	0.999151516	0.000848484
SWITCH REED SPST 10-15AT	SW1	10.2	1	10.2	0.764864947	0.235135053
TAB1	TAB	0.038	1	0.038	0.999001858	0.000998142
Battery	BATT	0.003886	1	0.003886	0.999897881	0.000102119
Packaging	PK1	0.6	1	0.6	0.984355664	0.015644336
Soldering	Sld	0.0002	1	0.0002	0.999994744	5.25599E-06

Total Failure Rate of System (λ_{sys}) = 14.1 failures/10⁶ hours
MTTF ($1/\lambda_{sys}$) = 70651 hours (8 years)
System Reliability R(t) = exp(- λ t) 68.9% for 3 years
78% for 2 years
88.3% for 1 year

Fault Tree Analysis of failure modes are as follows;

3.1. FTA (Fault Tree Analysis) - Temperature Sensor Failure

This is the mode of failure where only the temperature sensor fails and other parts of the circuit are working normally. This behavior is noticed when recorded data is plotted in post-processing software. When temperature sensor or temperature

sensing circuitry stopped responding, a flat line is observed throughout the recorded data which is an indication of failed sensor reading. The fault Tree of such a failure event is as follows in Figure 12;

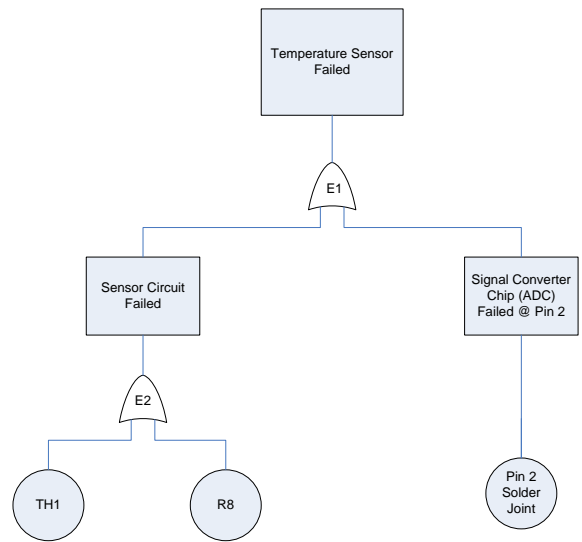


Figure 12 – FTA for Temperature Sensing Circuit Failure

The analysis of the tree is conducted by expressing the top event as a Boolean algebraic equivalent of the tree itself. The top event “E1” is the union of 02 basic events, E2 and Pin 2.

For the above failure event,

$$P(\text{temperature sensor failing}) = P(E2) + P(\text{Pin 2})$$

$$= P(\text{TH1}) + P(\text{R8}) + P(\text{Pin 2})$$

Inserting the values from Table 2, we get probability of failure of event E1;

$$P(E1) = 1.1\%$$

3.2. FTA - Pressure Sensor Failure

This mode of failure is described when only pressure readings are not obtained due to pressure sensor circuitry failure, which also includes amplifier and signal converter. This phenomenon is also observed, as temperature sensor failure, as a flat line showing an infinite value of pressure in the data. The fault tree of such a failure event is shown in Figure 13;

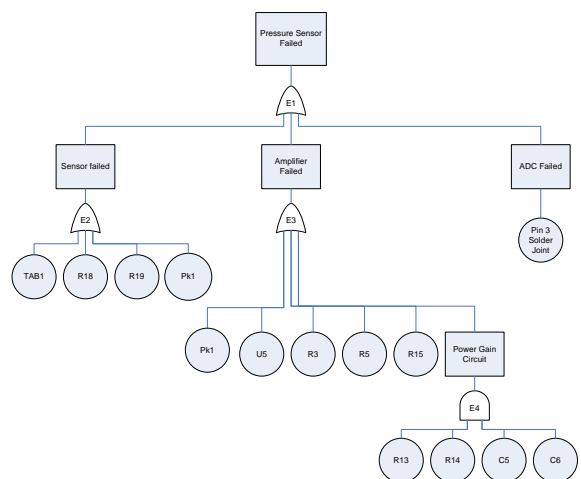


Figure 13 – FTA of Pressure Sensing Circuit Failure

3.3. FTA - Communications Failure

This mode of failure results in no communication with the data recorder when an attempt is made to download recorded data. The Fault tree for such a failure event is plotted and shown in Figure 14.

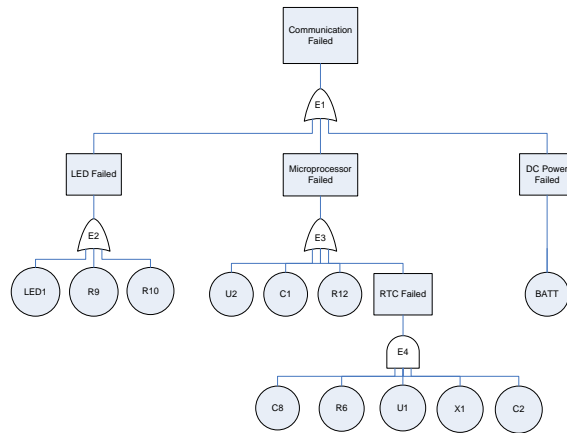


Figure 14 – FTA for Communications Circuit Failure

3.4. FTA - Power Failure

This mode of failure occurs when the total power of the system fails. The fault tree for such a failure event is described below in Figure 15;

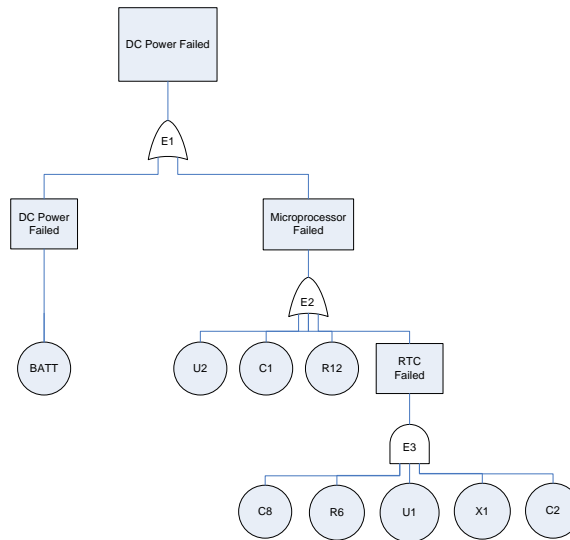


Figure 15 – FTA for Power Circuit Failure

A summary of FTA results are captured in Table 3.

Table 3 – Summary of FTA Analysis

Failure Mode	Probability of Failure
Temperature sensor and circuit failure	1.1%
Pressure sensor and circuit failure	3.64%
Communication circuit failure	0.65%
Power circuit failure	0.53%

It can be seen that the probability of pressure sensor circuit failure is the highest amongst all.

4. Failure Mode Analysis: Experiments and Simulation

In Data Recorder tags, all electronic components along with the battery and sensors are moulded with polyurethane that provides protection. Two kinds of polyurethanes are used to encapsulate the electronics, one is clear and hard with high tensile strength and the other is soft rubber like which is dark in colour with low yield strength. The latter is used to cover the

sensitive pressure sensor so that it remains protected from handling. The pressure sensor needs to be able to sense the compression of the soft polyurethane membrane as it deflects under the effect of pressure. Figures 16-17 shows details of the constructed tag under study.

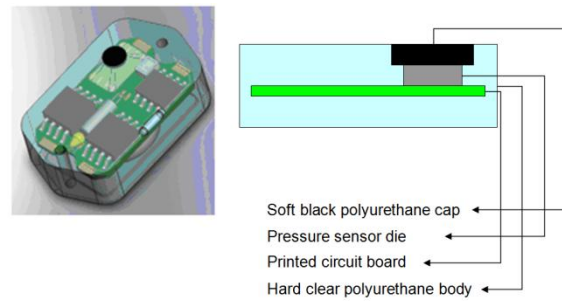


Figure 16 – Anatomy of the Data Recorder Tag showing Polyurethane Body

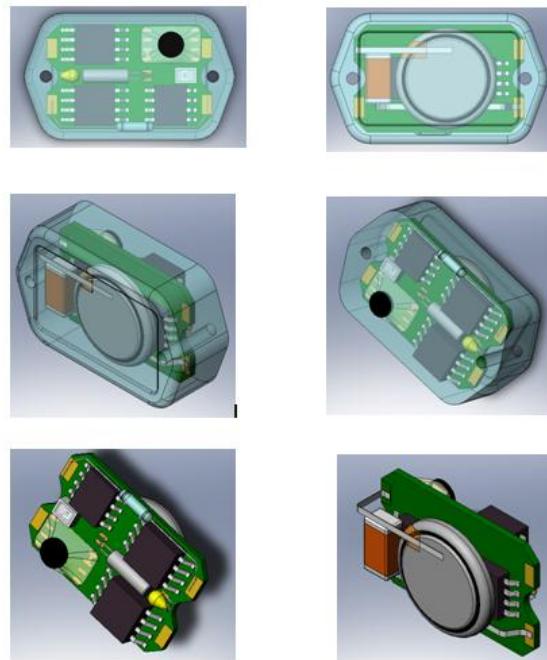


Figure 17 – 3D Assembly Model of Data Recorder Tag Under Study

It is suspected that water leaks through the interface between the black and the transparent urethane and causes damage to the pressure sensor and/or battery. This results in either only pressure sensor failure or adds to rapid discharge of the battery. To investigate water penetration through the plastic body, structural analysis of the data recorder is conducted both experimentally and numerically using finite element analysis. The focus of the structural analysis is on the stresses at the interface of the two types of polyurethanes used to package the tag. Since both types of the polyurethanes have different coefficients of thermal expansion, this may give rise to high residual stresses at the interface of the two materials and thus result in a lower tensile strength for the packaging. It is important to know if the materials used for encapsulation are strong enough to sustain such pressures. Any structural failure can cause water to ingress and cause damage to the electronics inside. Structural stress analysis is conducted using the finite element method at different pressures and results were compared with experimental analysis.

4.1. Structural Analysis

Pressure experiments are conducted to test these tags under such pressures and to determine the design limitations. The tags were placed in a hydraulic pressure vessel capable of creating pressures up to 4500 psi. The first few data-recorder tags were subjected to pressures of 700, 1420 and 2800 psi for a period of 1 minute each. In another experiment, tags were subjected to the same pressures mentioned above for a period of 5 hours each to observe creep effects. Data recorder tags are designed for marine animal study, which live in water and can reach depths of 1000 meters in cold oceans. Under such pressures, moulding compounds which encapsulate the electronics are subjected to pressures which create compressive stresses on the surface of the data recorder and has a potential to damage the soft and hard polyurethane body.

A few test specimens were made, as shown in Figure 18, using the same manufacturing procedure used for the manufacture of the actual data-recorder tag. These test samples were moulded with moisture absorption test paper (Cobalt Chloride test strip), which turns white in colour when moisture is absorbed. The moisture tests strip replaces the actual circuit board and electronic components to keep cost of test specimens low. Tag size and dimensions were exactly the same as the actual product.



Figure 18 – Fully Moulded Test Samples in Silicone Moulds

4.2. Pressure Experiments

Test specimens were placed inside the hydraulic pressure vessel, as shown in Figure 19, and subjected to three pressures, 700, 1420 and 2800 psi for only 1 minute. In the second stage of experiments, the same pressures were applied for 5 hours to create creep affects.



Figure 19 – Hydraulic Pressure Vessel

After each applied pressure for the specific time, samples of data recorder tags were taken out of the vessel and inspected under the microscope for any cracks and visible damage. Table 4 shows the results at all applied pressure ranges.

Table 4 - Pressure Tests Results

Applied Pressure	Duration: 1 minute	Duration: 5 hours
700psi	no damage noticed	no damage noticed
1420psi	no damage noticed	no damage noticed
2800psi	no damage noticed	damage noticed

No damage was observed when samples were subjected to 700, 1420 and 2800 psi pressure for 1 minute. But when same pressures were applied continuously for 5 hours, micro-cracks were observed on the soft black polyurethane circular cap only. The cracks are not only in the middle of the soft polyurethane but also on the edges, which is the interface of soft and hard polyurethane. There was no damage observed on the hard clear polyurethane material. Figures 20 and 21 show cracks on the circular cap.

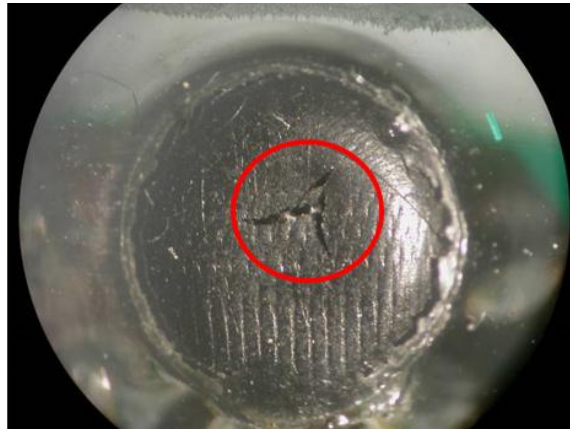


Figure 20 – Micro Cracks on Soft Polyurethane, Sample 1

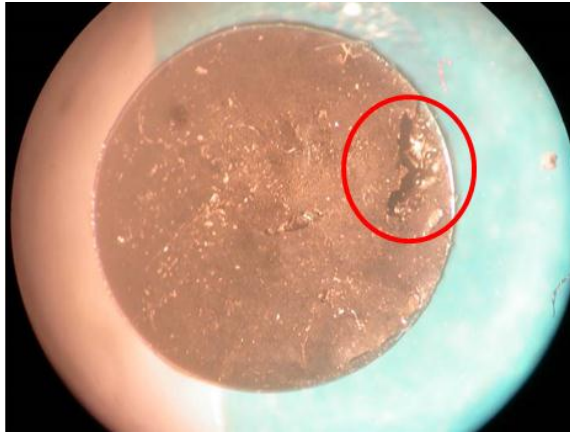


Figure 21 – Micro Cracks on Soft Polyurethane, Sample 2

4.3. FEA (Finite Element Analysis) Simulation of Pressure

To validate the experimental results, FEA simulation is conducted using commercially available finite element package software. The same pressure values were used in FEA simulation as used in pressure experiments. Material properties were obtained from the datasheets supplied by the manufacturer and presented in Table 5.

Table 5 - Material Properties of the Encapsulants

Material Properties	Soft Polyurethane (Black)	Hard Polyurethane (Clear)
Elastic Modulus (N/m ²)	9E06	300E07
Poisson's Ratio	0.49	0.39
Tensile Strength (N/m ²)	6.89E05	1.99E07
Yield Strength (N/m ²)	9E06	300E07
CTE (/K)	0.00067	0.00063
Thermal Conductivity (W/m.K)	0.14	0.189
Specific Heat (J/kg.K)	1	1

Since the soft polyurethane material, which is used to create the circular cap for the pressure sensor, resists flow in the linear direction yet sustains large deformations, it is defined as non-linear visco-elastic material as the relation between stress and strain is non-linear. This is needed for creep analysis, which is the application of pressure for a long period of time. Therefore, the study is divided into two parts, one for static load analysis and the other for creep analysis.

From previous pressure experiments as described above, we learned that there is no damage on the hard polyurethane surface. It is mainly due to the fact that the hard polyurethane has a very high tensile and yield strength compared to soft

polyurethane, $1.99E07 \text{ N/m}^2$. Therefore, to reduce the simulation processing time, the model size is reduced to only soft polyurethane, which means; only soft polyurethane is being modeled instead of modeling the whole structure. Figures 22 and 23 show the soft polyurethane circular cap as modeled in FEA.

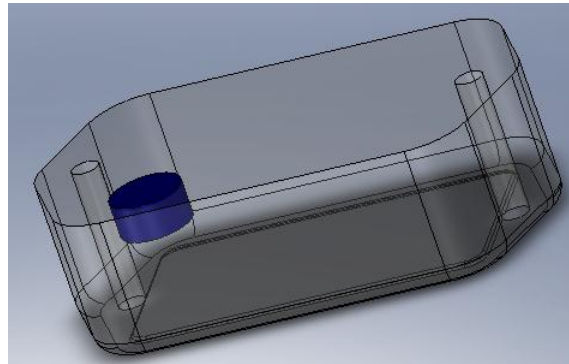


Figure 22 - Sketch of Data Recorder Tag Showing Only Two Polyurethane Moulding Compounds

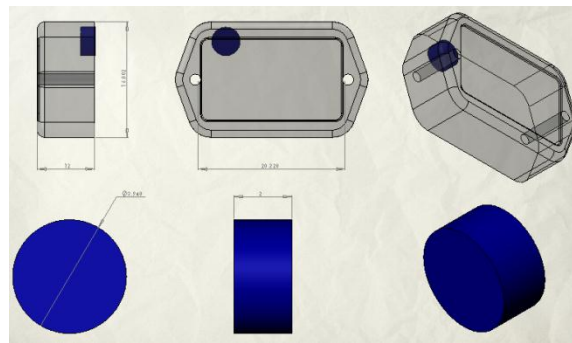


Figure 23 - Dimensions of Data Recorder Tag and Soft Polyurethane Compound

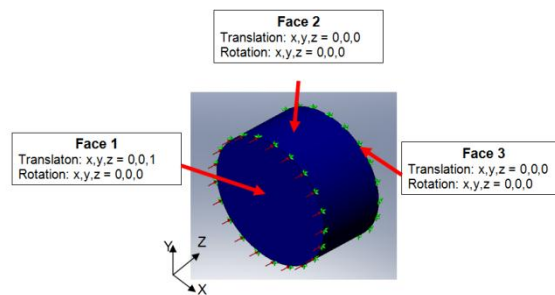


Figure 24 - Soft Polyurethane Compound Model Showing Restraints and Pressure

Figure 24 shows the boundary conditions for the model. Face 1, which is considered as the top face of the component, is subjected to pressures, whereas, Face 3, is the bottom face of the component sitting on top of the pressure sensor. Face 1 is allowed to have translation in z-direction but translation in x and y direction is restricted. Rotation is also restricted in all directions for Face1. However, Faces 2 and 3 are restricted for translation and rotation in all directions.

Using the model as shown in Figure 24 and material properties as described in Table 5, pressure simulation studies were conducted by applying 1420 psi and 2800 psi pressures to Face 1. Results were obtained for Von-Mises stresses, displacements and strains. Results of FEA simulation for 1420 psi pressure are shown in Figures 25 and 26. It can be noted from Figure 25 that the maximum stress value, $2.8E06 \text{ N/m}^2$, at 1420 psi is under the yield strength of the material which is $9E06 \text{ N/m}^2$.

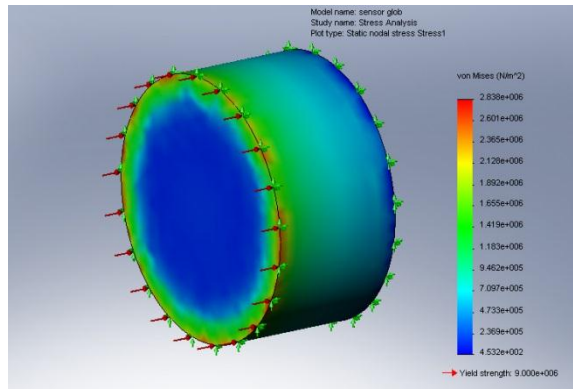


Figure 25 - Von Mises Stresses when 1420 psi pressure is applied

The maximum displacement is observed in the center of the circular cap, Figure 26. This behaviour is expected as the cap is constrained to deflect from sides, Face 2, so the maximum deflection from the center is in the z-direction and of magnitude of 0.19 mm.

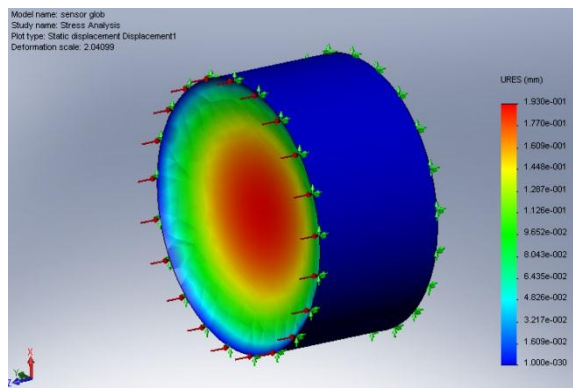


Figure 26 - Displacement when 1420 psi pressure is applied

Results of FEA simulation for 2800 psi pressure are shown in Figures 29 and 30. It can be noted from Figure 27 that the maximum stress value, 5.5E06 N/m², at 1420 psi is under the yield strength of the material which is 9E06 N/m².

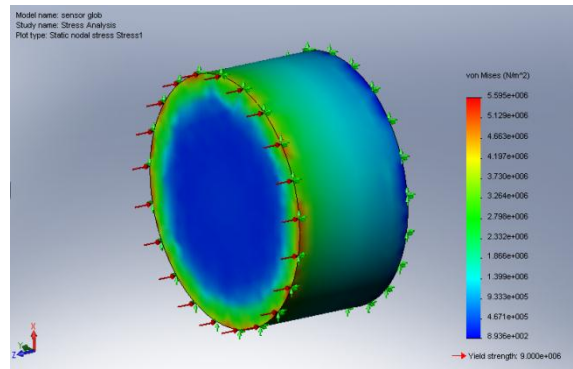


Figure 27 - Von Mises Stresses when 2800 psi pressure is applied

The maximum displacement is observed in the center of the circular cap, Figure 28. This behaviour is expected as the cap is constrained to deflect from sides, Face 2, so the maximum deflection from the center is in the z-direction and of magnitude of 0.38 mm.

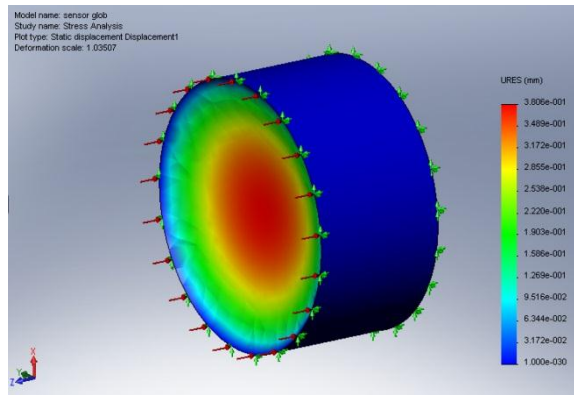


Figure 28 - Displacement when 2800 psi pressure is applied

Compared to yield strength of the material, $9E06 \text{ N/m}^2$, the maximum value of stress is below the yield strength of the soft polyurethane circular cap at both applied pressures. The direction of deflection matches with the observations made in previous studies of pressure experiments. Since the maximum stress value is under the yield strength of the material, the conclusion can be drawn that the material did not fail under applied pressure values. Pressure experiments that showed cracks on the soft polyurethane circular cap when pressure of value 2800 psi was applied for a longer period of time is due to creep affects and mainly due to the visco-elastic nature of the material. To study creep affects through FEA and also to determine the time it takes the material to achieve stress greater than its yield strength, a FEA study was designed and conducted as described below. Keeping pressure at a constant value of 1420 psi, 5 simulations were run by changing time from 1 hour to 5 hours. Figure 29 shows the Von-Mises stress distribution when a pressure of 1420 psi is applied for 5 hours. The value of maximum stress, $5.1E06 \text{ N/m}^2$, is under the yield strength of the material, which is $9E06 \text{ N/m}^2$. Stress values have changed significantly compared to the static stress analysis study done in the previous section.

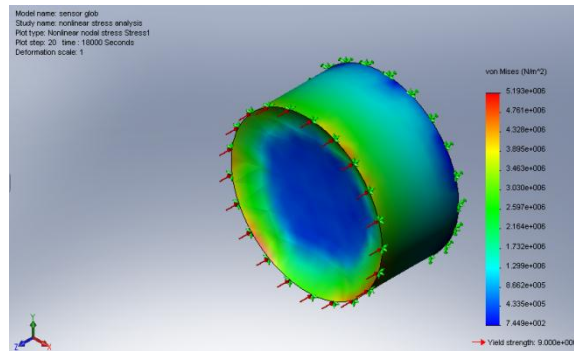


Figure 29 - Von Mises Stresses when 1420 psi pressure is applied for 5 hours

The maximum displacement after 5 hours at 1420 psi is 0.4 mm. The maximum deflection is at the center of the circular cap as shown in Figure 30.

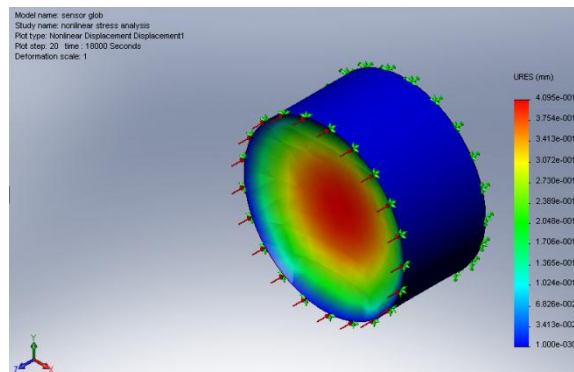


Figure 30 - Displacement when 1420 psi pressure is applied for 5 hours

Keeping pressure at a constant value of 2800 psi, 5 simulations were run by changing time from 1 hour to 5 hours. Figure 31 shows the Von-Mises stress distribution when pressure of 2800 psi is applied for 5 hours. The value of maximum stress,

1E07 N/m², is greater than the yield strength of the material, which is 9E06 N/m². High stress values will yield in deforming the circular cap permanently and failure can be seen in the form of cracks.

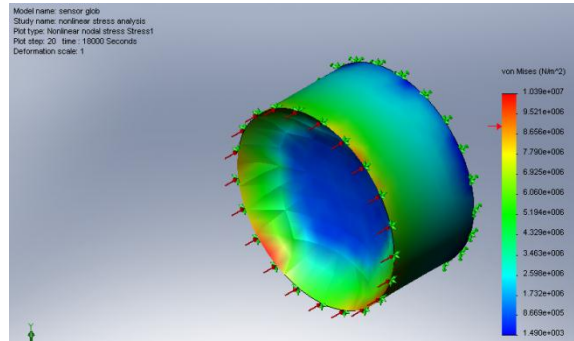


Figure 31 - Von mises Stresses when 2800 psi pressure is applied for 5 hours

The maximum displacement after 5 hours at 2800 psi is 0.81 mm. The maximum deflection is at the center of the circular cap as shown in Figure 32.

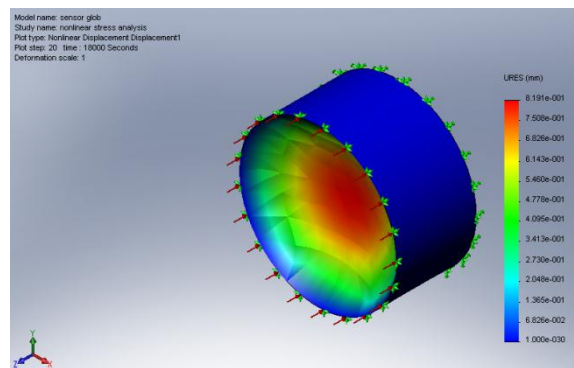


Figure 32 - Displacement when 2800 psi pressure is applied for 5 hours

Compared to the yield strength of the material, 9E06 N/m², the maximum value of stress exceeds the yield strength of the soft polyurethane circular cap when the pressure value of 2800 psi is applied for 5 hours. Deflections along the z-direction increase as the applied pressure and time increases. Large strain combined with the high stress value after 5 hours of 2800 psi pressure can cause this material to deform permanently and be the reason for cracks, which open the path for water to enter the plastic polyurethane body and reach the electrical circuit.

4.4. Summary of Structural FEA

Summarizing the results from static stress and creep analysis in Table 6, it is clear that when 2800 psi pressure is applied for 5 hours, stresses exceed the yield strength of the material and thus result in cracks which matches to results obtained from physical pressure experiments shown in Figures 31 and 32.

Table 6 - Summary of Static Stress and Creep Analysis

	Static Stress Analysis		Creep Analysis (5 hours)	
	1420psi	2800psi	1420psi	2800psi
Von Mises Maximum Stress (N/m ²)	2.8E06	5.12E06	5.19E06	1.039E07
Displacement (mm)	0.19	0.38	-0.409	-0.819

From the animal behaviour as observed through recorded data and published studies, it is not normal for any animal to dive to depths of 2800psi (1970 meters) and stay there for such a long time of 5 hours. The normal dive pattern of most deep diving animals is between 3 to 9 minutes.

Therefore, it can be concluded that the design of the data-recorder tag is good for the applications where the pressure, even as high as 2800 psi, is applied for a short period of time, not for 5 hours as in experiment and simulation. Recorded data from the tags that failed under the packaging failure mode show that animal diving patterns was closer to 1500 psi (1000 meters) and also no physical damage was noticed on the casing of the failed tags, meaning no cracks. This means that the water penetration which is the effect of the packaging failure was not caused by high stresses or openings through the plastic polyurethane body but could be due to moisture diffusing through the polyurethane material.

Therefore, further investigation of the packaging failure is required from a moisture diffusion perspective since it has been established that polyurethane packaging is strong enough to sustain a high pressure, 2800 psi, when applied for a few minutes, which is the normal behaviour of the marine animals.

5. Moisture Diffusion in Electronic Packaging Materials

The presence of moisture in plastic packaging alters thermal stress through alteration of thermo-mechanical properties. For example; change of elastic modulus, shear strength and glass transition temperatures. Moisture also;

- Induces hygroscopic stress through differential swelling
- Reduces interfacial adhesion strength
- Induces corrosion
- Acts as an unwanted resistance when present between the two nodes of component and result in lowering the resistance

The sketch shown in figure 33, shows the possible diffusion paths of moisture in the plastic encapsulated body of the tag.

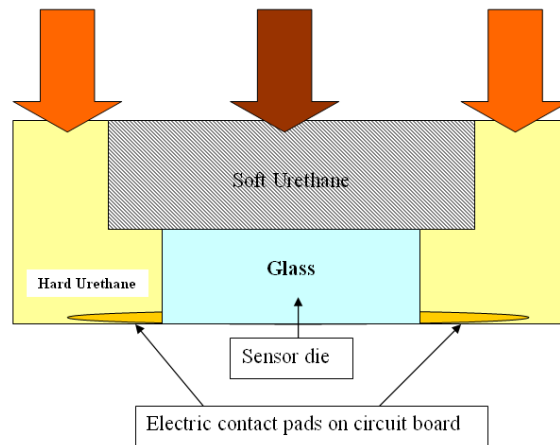


Figure 33 - Sketch Showing Diffusion Paths for Water through Hard and Soft Polyurethane Materials

5.1. Analytical Approach

Fick's second law, Equation (9), is used in non-steady or continually changing state diffusion which is when the concentration within the diffusion volume changes with respect to time.

$$\frac{1}{D} \frac{\partial C}{\partial t} = \frac{\partial^2 C}{\partial x^2} + \frac{\partial^2 C}{\partial y^2} + \frac{\partial^2 C}{\partial z^2} \tag{9}$$

Where;

C = concentration of diffusing substance (g/cm³)

D = diffusion coefficient (cm²/sec)

x,y,z = dimensions in x, y and z direction (cm)

Polymeric packaging materials transport moisture primarily by diffusion, although secondary effects such as surface tension and pressure driven flows may also contribute. Moisture transport strictly by diffusion is modeled using the standard transient diffusion as per Fick's second law. Wong, Koh, Lee and Rajoo (2002) [3] showed that the Crank's equation (Mathematics of Diffusion, 1956), can be modified into Equation (10) to calculate the diffusion coefficient for isotropic materials.

$$\frac{M_t}{M_\infty} = 1 - \frac{8}{\pi^2} \sum_{m=0}^{\infty} \frac{1}{(2m+1)^2} \exp\left[\frac{-D(2m+1)^2 \pi^2 t}{h^2}\right] \quad (10)$$

Where;

h = total sheet thickness (mm)

M_t = total mass of the diffusing substance absorbed at time t

M_∞ = Equilibrium mass of the absorbed substance

D = diffusion coefficient (mm²/hour)

Since the Equation (10) assumes that there is no diffusion from the edges of the specimen or it is only true for a large aspect ratio, Equation (11) is the correction factor needed to compensate diffusion in the z-direction, as prescribed by Wong, Koh, Lee and Rajoo (2002)[3]

$$D_z = C_f \times D_{1-D} \quad (11)$$

For a square specimen,

$$C_f = \frac{1}{1 + \left(\frac{2z}{x}\right)^2} \quad (12)$$

Where;

C_f = correction factor

Z = thickness of specimen (mm)

X = length/width of the specimen

Zhou, Coffin and Arvelo (2006) [4] suggested another correction factor, as shown in Equation (13).

$$D_c = D \left(1 + \frac{h}{l} + \frac{h}{w}\right) \quad (13)$$

Where;

D = diffusion coefficient neglecting edge effect (mm²/hour)

D_c = diffusion coefficient including edge effect (mm²/hour)

h = height or thickness of the specimen (mm)

l = length of the specimen (mm)

w = width of the specimen (mm)

Using Crank's equation (Mathematics of Diffusion, 1956), shown in Equation (14);

$$\frac{C(x,t)}{C_\infty} = 1 - \frac{4}{\pi} \sum_{n=0}^{\infty} \frac{(-1)^n}{2n+1} \exp\left[\frac{-D(2n+1)^2 \pi^2 t}{4l^2}\right] \frac{\cos(2n+1)\pi x}{2l} \quad (14)$$

Where;

l = half thickness of sheet (mm)

D = Diffusion coefficient (mm²/hour)

t = time (hour)

C = concentration of diffusing substance in time t (g/mm³)

C_∞ = Saturated concentration of the absorbed substance (g/mm³)

In the initial stages of absorption where $M_t/M_\infty < 0.5$ and assuming a constant diffusion coefficient, D , the above equation can be approximated to Equation (15) as shown by Wong, Koh, Lee and Rajoo (2002) [3].

$$\frac{M_t}{M_\infty} = \frac{4}{h} \sqrt{\frac{Dt}{\pi}} \quad (15)$$

If absorption data is plotted with M_t/M_∞ as a function of $(t/h^2)1/2$ and exhibits linear behaviour for $M_t/M_\infty < 0.5$, the diffusion coefficient can be determined by re-arranging Equation (15) to Equation (16);

$$D = \frac{\pi}{16} \left[\frac{M_t / M_\infty}{\sqrt{t} / h} \right]^2 \quad (16)$$

The diffusivity, D , can now be experimentally determined using absorption data (M_t/M_∞) by weight gain experiment as prescribed in ASTM D570 method.

Once the diffusivity coefficient is known, the theoretical Fickian curve can be plotted with the experimental data to see if the absorption is Fickian or not. This can be done by using the value of “ D ” calculated from weight gain experiments and plotting the graph with different time values. Equation (17) can be used;

$$\frac{M_t}{M_\infty} = 1 - \exp \left[-7.3 \left(\frac{Dt}{h^2} \right)^{0.75} \right] \quad (17)$$

Figure 34 represents an example of the graph plotted between M_t/M_∞ and $t1/2$, dotted marks are the data from experiment and the continuous line is a Fickian curve.

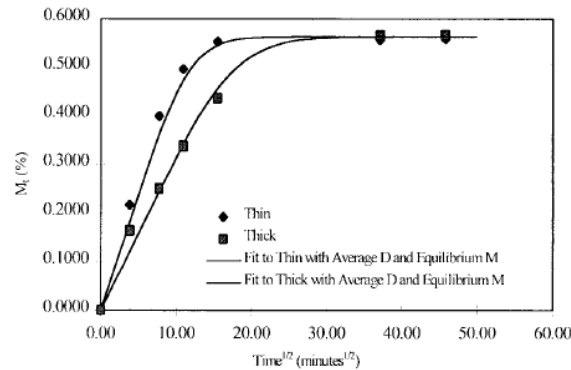


Figure 34 - Example of a Fickian Curve

For very prolonged times the curve becomes non-fickian, therefore, the diffusion coefficient is calculated by considering only the linear part of the curve. For materials showing non-fickian behaviour, Wong, Koh, Lee and Rajoo (2002)[3] suggested to use the following Equation (18);

$$t_{99\%} = \frac{0.45 h^2}{D} \quad (18)$$

Where;

$t_{99\%}$ = time to approach 99% saturation (hours)

h = height or the thickness of the specimen (mm)

D = diffusion coefficient (mm²/hour)

The 99% saturation approach helps to define the limit of Fickian diffusion hence eliminate error caused by non-fickian sorption. Datasheets obtained from the materials manufacturer provided the information regarding water absorption (M_t/M_∞) using ASTM D570 test method, as shown in Table 7. The values provided in Table 7 were used to calculate the diffusion coefficient using Equation (16).

Table 7 - Water Absorption Properties from Polyurethane Datasheet

	Soft Polyurethane	Hard Polyurethane
Water Absorption, % (168 hours at 25°C) ASTM D570	0.3	0.2

Inserting the values of M_t/M_∞ in Equation (16) for soft polyurethane, we get;

$$D = 4.20 \times 10^{-4} \text{ mm}^2/\text{hr}$$

Using equation 18, moisture diffusion ingress rate can be calculated.

$$t_{99\%} = 4285.71 \text{ hours} = 178.5 \text{ days}$$

Using equations 16 and 18 again for hard polyurethane, we get;

$$D = 1.07 \times 10^{-3} \text{ mm}^2/\text{hr}$$

$$t_{99\%} = 60560.74 \text{ hours} = 2523.36 \text{ days} = 6.913 \text{ years}$$

The results are summarized in Table 8 below;

Table 8 - Diffusion Coefficients for Polyurethanes, Soft and Hard

	Soft Polyurethane	Hard Polyurethane
Diffusion Coefficient, D (mm ² /hr)	4.20×10^{-4}	1.07×10^{-3}
$t_{99\%}$ (days)	178.5	2523.36

Referring to Table 8, it takes approximately 6 months for the soft polyurethane circular cap to fully saturate with water whereas 7 years for hard polyurethane. Considering it takes 7 years to diffuse through the hard polyurethane, it is not considered for the FEA simulation study. Only the soft polyurethane circular cap was modeled in the next section as it diffuses in 6 months which can be the cause of failures in the tag.

5.2. Finite Element Analysis of Moisture Diffusion

Since the Fick's moisture diffusion equation follows the same governing differential equation as the diffusion of heat (Fourier,1822), with a change of the dependent variable, temperature, with moisture concentration and the thermal diffusivity with moisture diffusivity, commercially available heat transfer simulation software can be used to solve transient moisture diffusion problems. However, a unique problem arises in the diffusion of moisture. Since D is constant for a particular material, for bi-material analysis, interfacial concentration discontinuity cannot be analyzed. An interfacial discontinuity results where two materials having different saturated concentrations are joined. To use heat transfer simulation software for moisture diffusion simulation, manipulation in defining material properties is required. This is done by replacing thermal conductivity of the material with moisture diffusion coefficient, which was calculated in the previous section, and defining density and specific heat to unity. The method is prescribed by Yoon, Han and Wang (2007)[5] and shown in Table 9.

Table 9 - Variables Map for FEA Simulation

Heat Transfer (Temperature, T)	Moisture Diffusion (Moisture Concentration, C)
ρ , density (kg/m ³)	1
k, Conductivity (W/m.K)	D
c_p , Specific Heat (J/kg.K)	1

As shown in Figure 35, Face 1 is exposing the face of the circular cap where moisture is applied and therefore concentration on Face 1 is set to 1, meaning completely wet. Face 2 and 3 are defined as completely dry faces and concentration set to 0.

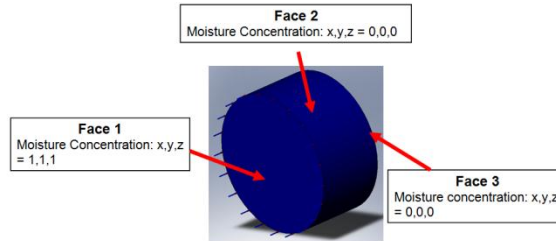


Figure 35 - Boundary Conditions for Moisture Diffusion FEA Model

Where;

C = 0 for complete dryness

C = 1 for saturated wetness

Following are the results of the moisture diffusion simulation as shown in Figures 36 to 39.

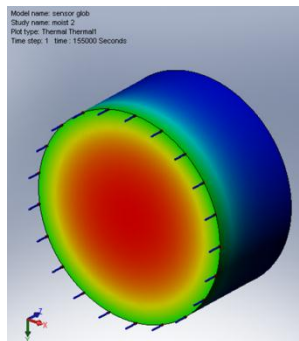


Figure 36 - Moisture Diffusion after 1.8 days

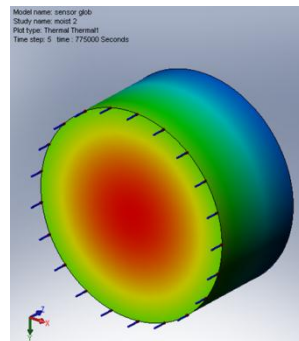


Figure 37 - Moisture Diffusion after 10 days

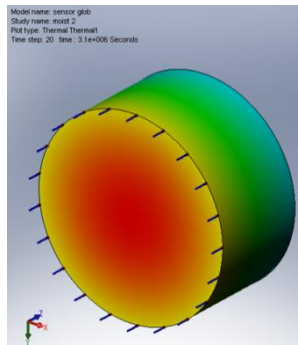


Figure 38 - Moisture Diffusion after 35 days

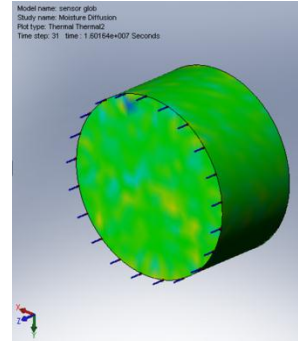


Figure 39 - Moisture Diffusion after 185 days

From the simulation results it is observed that it takes approximately 185 days for soft polyurethane to saturate 99%, which is close to the ingress rate result as calculated in the previous section thus validating the FEA model. Table 10 shows the result of moisture diffusion time obtained numerically and analytically.

Table 10 - Moisture Ingress Rate Results

Moisture Ingress Rate (Soft Black Polyurethane Circular Cap)	
Calculated	178 days
FEA	185 days

Moisture diffusion ingress rate is calculated and validated through finite element modeling. It takes approximately 6 months for soft polyurethane to saturate 99% with moisture, whereas approximately 7 years for hard polyurethane, as illustrated in Figure 40.

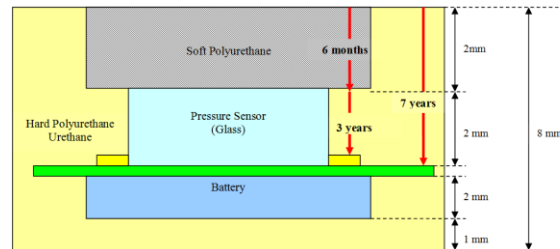


Figure 40 - Moisture Diffusion Time Through Two Polyurethane Materials

For moisture to reach the interconnect pads of the pressure sensor, when diffused through soft polyurethane material, which is at the bottom of the pressure sensor, it now needs to diffuse through hard polyurethane material of 2 mm in height as shown in Figure 40. All the electronic components in the tag, except the pressure sensor which is encapsulated with the soft polyurethane circular cap, can expect moisture to reach them through diffusion in 7 years. Whereas, the sensing surface of the pressure sensor can expect water, diffusing through the soft polyurethane material, in 6 months.

6. Conclusions

Considering the design life of the data recorder tag, which is from 2.5 years to 3 years, based on the maximum battery life, time for moisture to reach to the pressure sensor interconnect or the circuit board is 3.5 years, which is beyond the tag's design life. Therefore, it can be concluded that packaging design is good to protect the electronic components and electrical circuit from moisture and does not allow moisture to penetrate the polyurethane material during its life. The failures observed from the failure data analysis, which are categorized as "packaging failures", are all well within 1 year of the tag's mission life. This can happen if the manufacturing process of moulding the electronics in the two polyurethane materials is not in control.

An important factor that is not considered in the study is the interface of two polyurethane materials, soft and hard, which is adhesively bonded to each other. If this bond is compromised, it will open up a path for water to travel faster to the components on the circuit board. One of the important factors for this bond to be reliable is the contact area, which is created during the moulding process when hard and soft polyurethane material in liquid form is poured by hand. If the process is not controlled it can result in achieving a contact area which is beyond design specifications and cause the bond to break during small pressure applications. Smaller contact area can also cause moisture to diffuse faster than calculated previously. Another important interface is the bond between hard polyurethane and pressure sensor components which is made of glass material. There is no data available on the bond strength of these two materials but if compromised, along with the bond of soft and hard polyurethane will become an open channel for water to reach the electrical circuit and result in either short circuiting one or more electronic components or creating an excess discharge phenomenon, which leads to rapid discharge of the battery.

It is concluded that failures due to power, packaging and pressure sensors are related to each other. The power provided by the battery is enough to last it for at least 3 years and the structural analysis revealed that packaging is good to sustain pressures at 2000 meters deep in the ocean, as per the design. The root cause of the above mentioned failures are all related to moisture diffusion, diffusing through soft polyurethane material entering the body of the tag, either short circuiting the pressure sensor or creating low resistance between the two nodes of the pressure sensor connection pads resulting in rapid discharge of the battery, thus power failures.

7. References

1. Walker, Robert V., Siviridov, Vladamir V., Urawa, Shigehigo, Azumaya, T. (2007). Spatio-Temporal Variation in Vertical Distributions of Pacific Salmon in the Ocean. *North Pacific Anadromous Fish Commission Bulletin No. 4*, 193-201.
2. Department of Defense (1991). *Military Handbook MIL-HDBK-217: Reliability Prediction of Electronic Equipment*. Washington, D.C: DoD.
3. Wong, E.H., Koh, S.W., Lee, K.H., Rajoo, R. (2002). Advanced moisture diffusion modeling & characterization for electronic packaging. *Electronic Components and Technology Conference*, 1297-1303.
4. Zou, W., Coffin, J., & Arvelo, A. (2006). Reliability analysis on epoxy based thermal interface subjected to moisture environment. *IEEE Transactions*, 1082-1087.
5. Yoon, S., Han, B., Wang, Z. (2007). On moisture diffusion modeling using thermal-moisture analogy. *Electronic Packaging*, 129, 421-426.

Design for Reliability:

Improving Reliability of Plastic Encapsulated Ocean Technology Products by Understanding Moisture Ingress through FEA Simulation

Junaid Shafaat

Outline of Presentation

- Introduction
- Scope of Research
- Failure Data Analysis
- Top Two Failure Modes
 - Power Failure
 - Packaging Failure
- Conclusions
- Next Step

Biotelemetry

- *Telemetry is a technology that allows the remote measurement and reporting of information of interest.*
- **Biotelemetry** is the remote measurement of physiological data of living species
- It is used to study wildlife, and monitoring threatened species.
- Animals under study are fitted with instrumentation ranging from simple tags to cameras, GPS packages and transceivers to provide position and other basic information to scientists.

Applications of Tags



Courtesy of Lotek Wireless Inc.

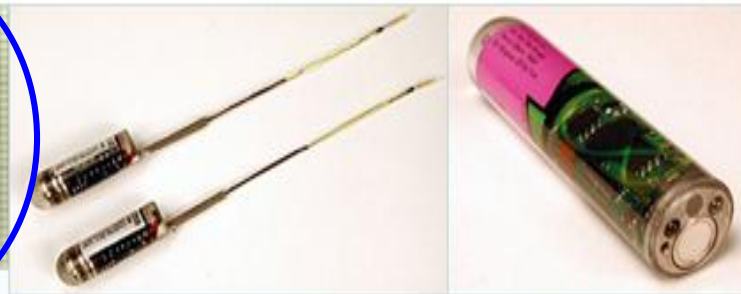
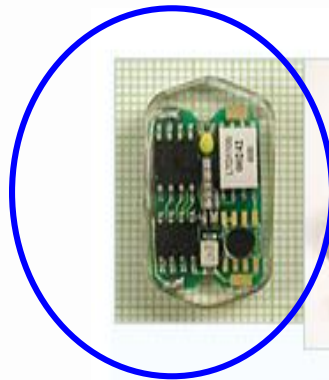
Biotelemetry Products



RF Transmitters



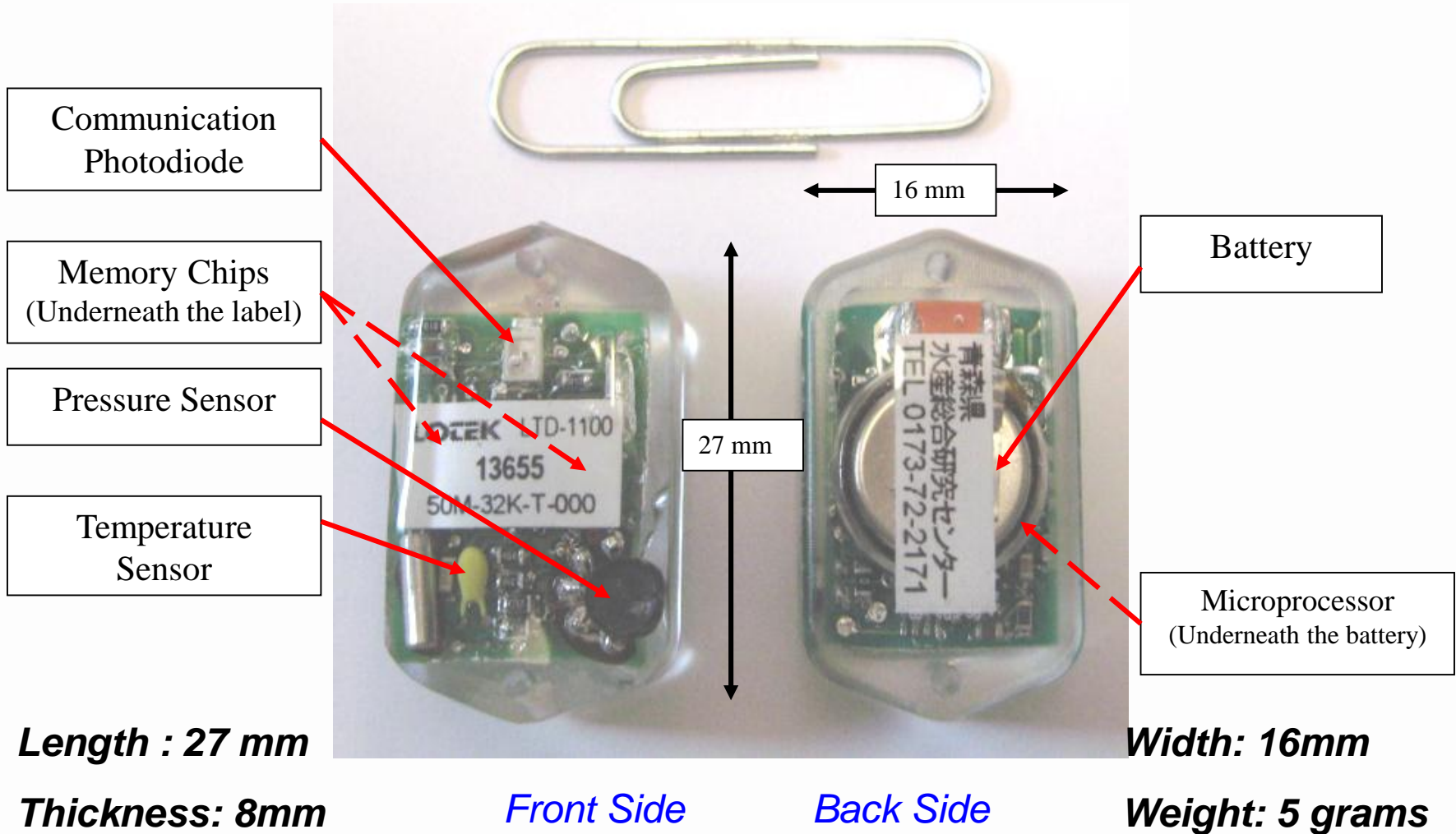
Acoustic Transmitters



Data-Recorder Tags

Courtesy of Lotek Wireless Inc.

Data-Recorder Tag



Scope of Research

- To determine Reliability of the data-recorder tags
- To determine failure rates and models
- To determine failure modes
- To find the root cause of failure modes

Failure Data Analysis

- 6 years of service data studied and summarized
- Failure criteria defined
- Failure modes identified

Deployed	Recovered	Failed	Good
5685	981	162	819
	17.3%	16.5%	83.5%

Failure Modes

Definition of Failure Modes:

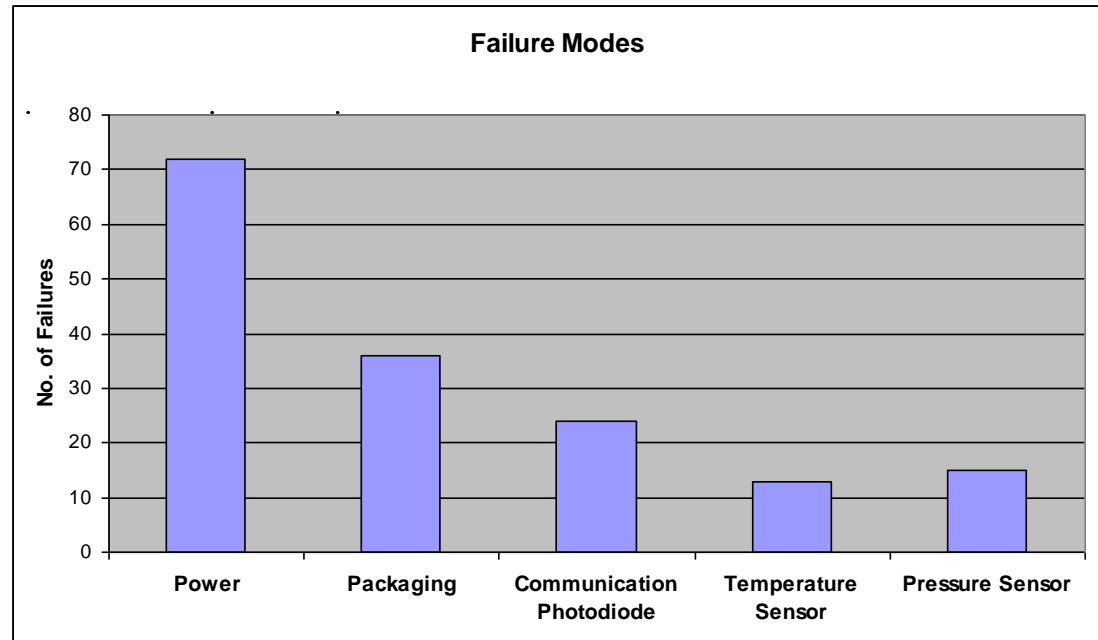
Power: Battery dies < 2 years

Packaging: External damage causing water to penetrate electrical circuits

Communication Photodiode: Failure of component, photodiode

Temperature Sensor: Failure of component, temperature sensor

Pressure Sensor: Failure of component, pressure sensor



Weibull Analysis

Time dependent failure rate

$$R(t) = e^{-(t/\theta)^\beta}$$

Where,

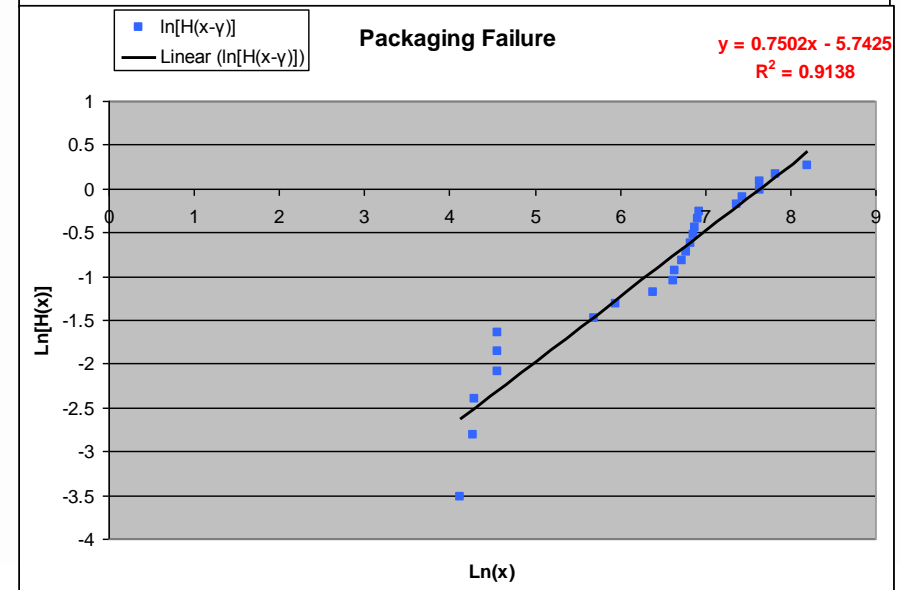
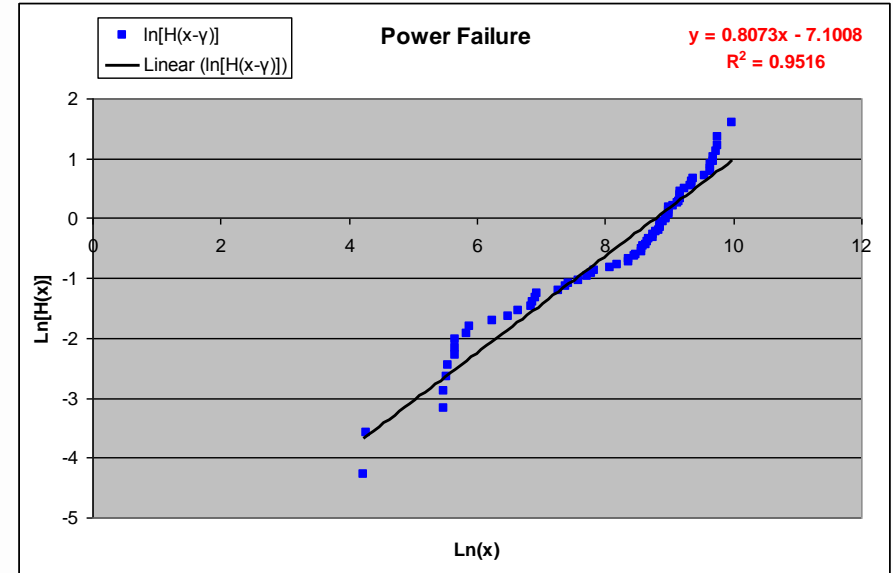
R(t) = Reliability at time t

t = time

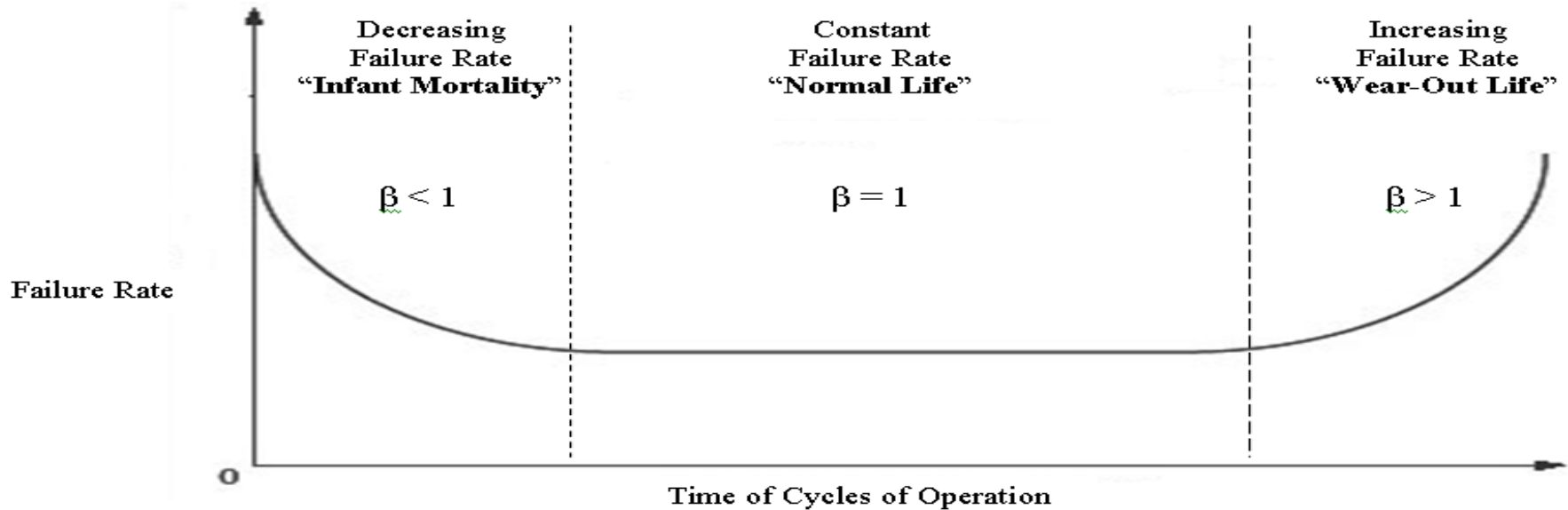
θ = Scale parameter or characteristic life. 63.2% failure will occur by the time $t = \theta$

β = shape parameter, defines shape of failure rate curve

- Decreasing failure rate as Scale Parameter, $\beta < 1$



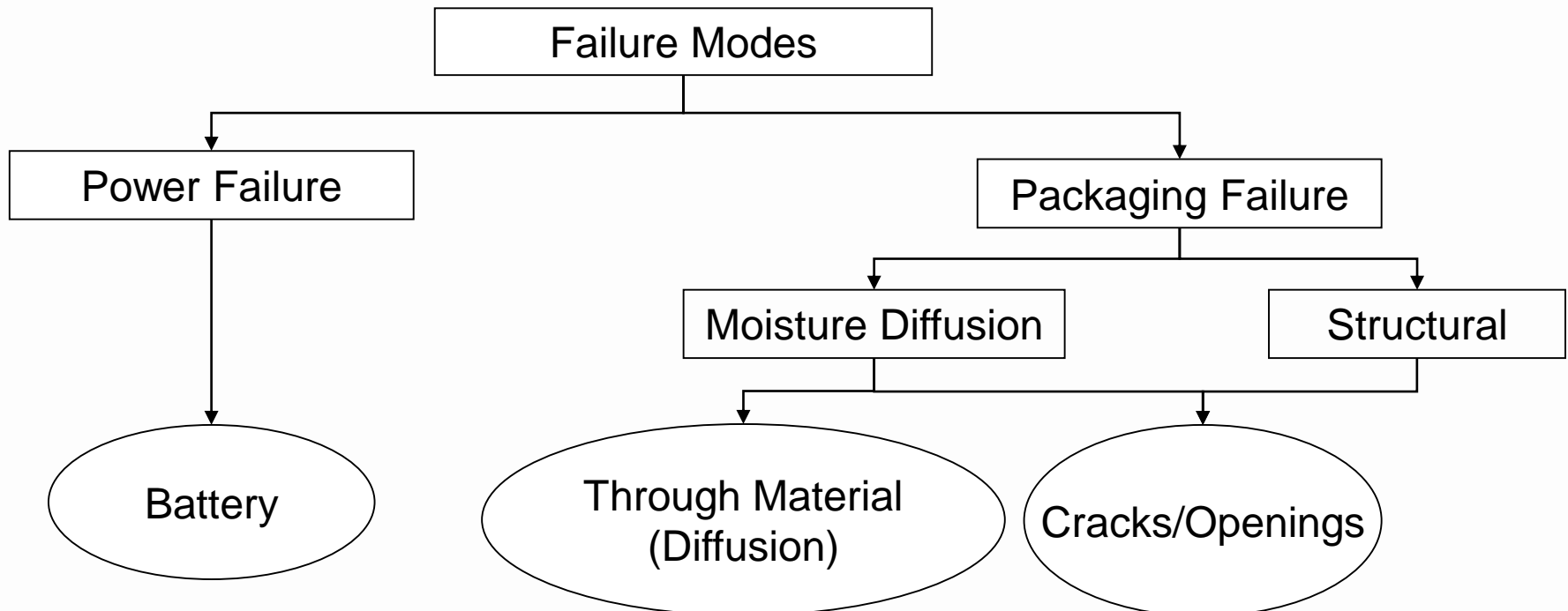
Weibull Analysis Results



Failure Mode	Shape Parameter	Scale Parameter	Result
Power	$\beta = 0.8073$	$\theta = 6606.03$	Infant Mortality
Packaging	$\beta = 0.7502$	$\theta = 2110.3$	Infant Mortality

Top Two Failure Modes

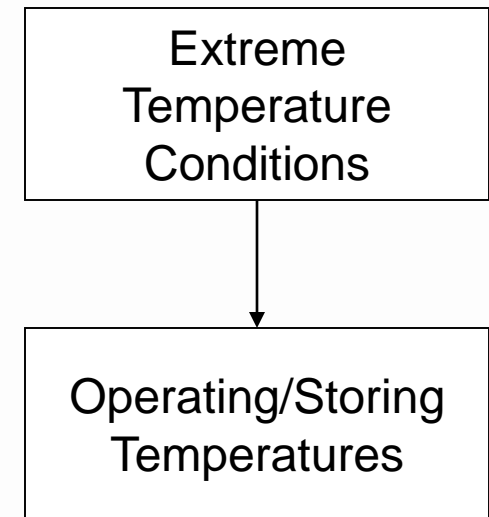
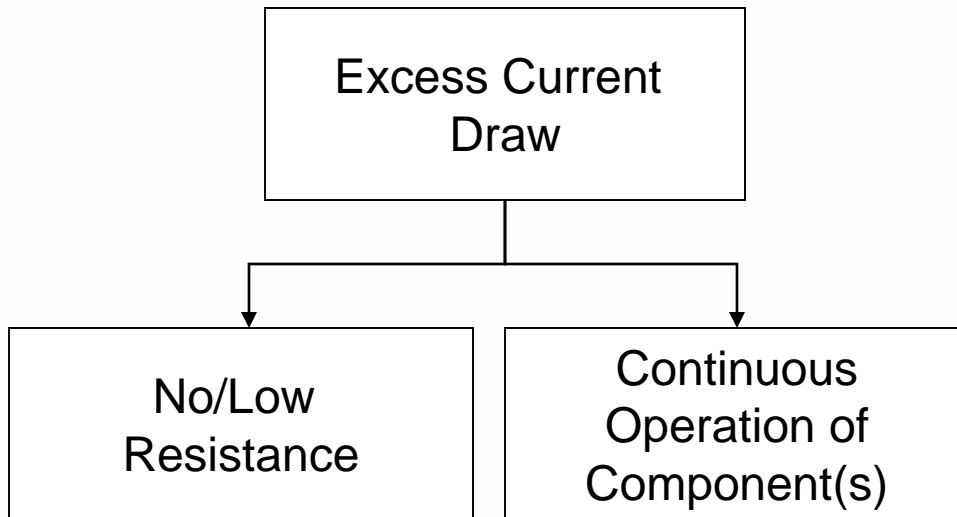
- **Power:** when battery dies before its designed life, < 2 years
- **Packaging:** water penetrating to electrical circuit, through;
 - Cracks or openings on the plastic body
 - Diffusing through encapsulating materials



Power Failures

Battery

- Premature battery failure is due to rapid discharge of battery
- Rapid discharge is due to;
 - Excess current draw from component(s) on the circuit board
 - Extreme temperature conditions

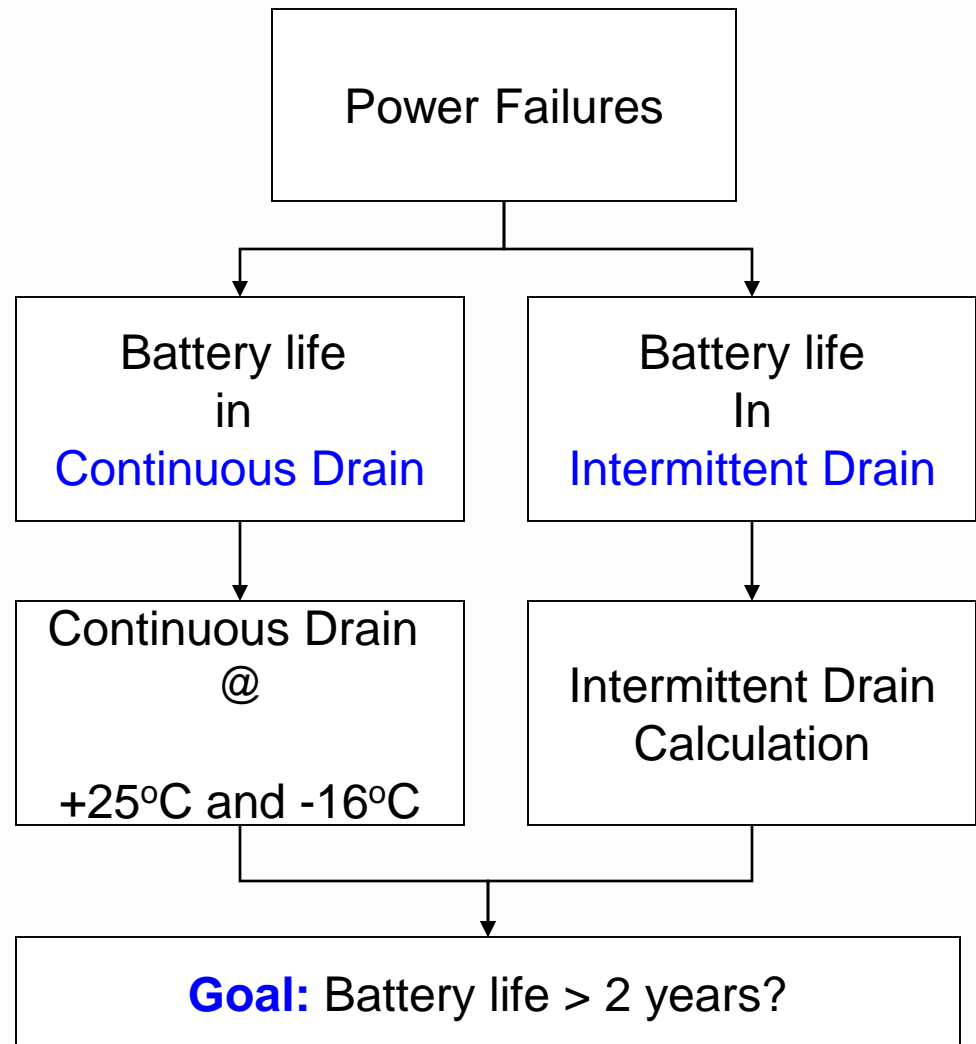


Experiments to Investigate Power Failures

Objective:

To determine true life of battery;

- At different temperature conditions
- At continuous and intermittent discharge conditions



Goal: Battery life > 2 years?

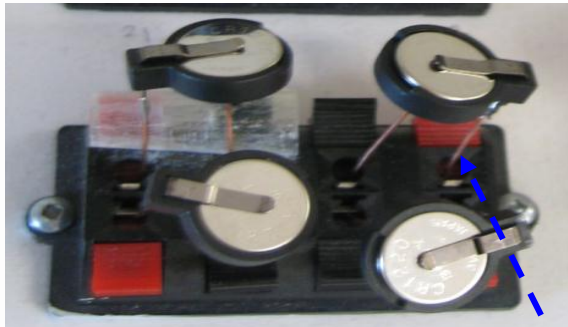
Battery Life in Continuous Drain Condition

- Continuous load of 18 k Ω is applied
- Voltage readings recorded using DMM till battery has reached its cut-off voltage of 2.0 V
- Experiment conducted at +25°C and repeated at -16°C

Raw



Tabbed



Load Resistor 18k Ω

Test Results

Continuous Drain

	Raw (n=15)	Tabbed	
		+25°C (n=15)	-16°C (n=5)
Total Discharge Hours =	259	257	211
Standard Deviation =	6.8	6.4	7.3
Coefficient of Variation =	2.6%	2.5%	3.5%
Standard Error =	3.10	2.79	10.74

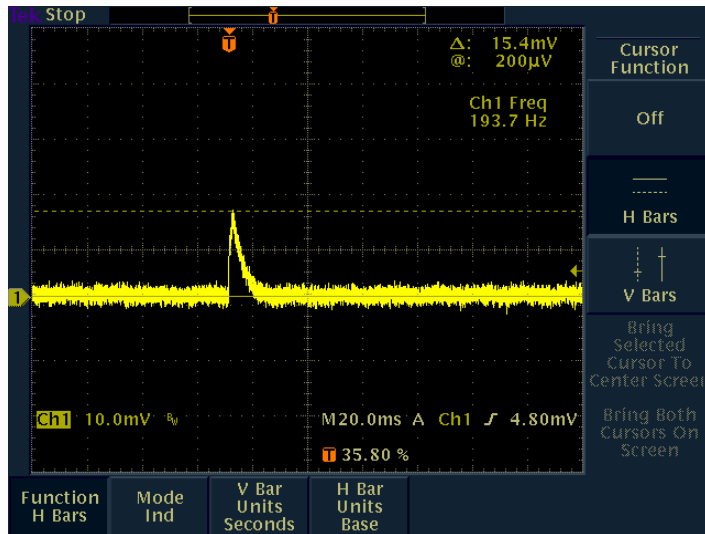
- Life of “Raw” and “Tabbed” cell is almost same
- Life of “Tabbed” cells at -16°C is approximately 45 hours less than cells tested at +25°C
- Results match to the datasheet provided by battery manufacturer

Battery Life in Pulsed Drain Condition

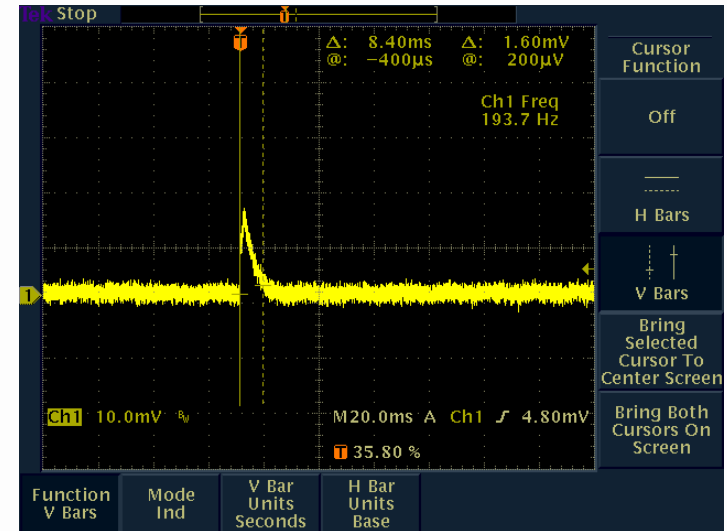
- Except for continuous “sleep current” all the other microprocessor activities are intermittent, i.e; “*Pulsed*”
- Pulsed conditions are due to following activities;
 - Sample
 - Data download
 - Reset
- Calculations of true battery life requires current measurements for each activity

Microprocessor Current Measurements

Time of Pulse at Sampling Activity



Current Draw at Sampling Activity

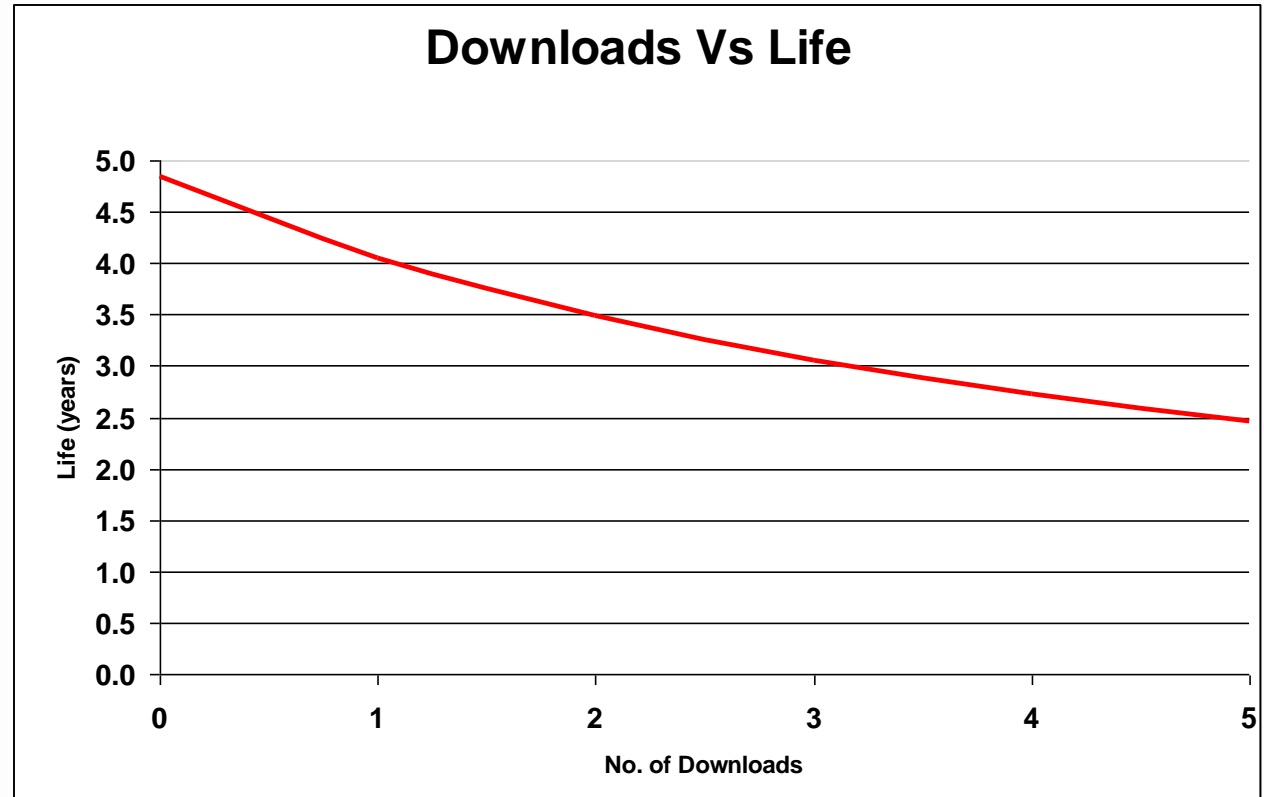


Pulse Activity	Current (uA)	Duration (sec)
Reset	840	0.124
Sample	154	0.84
Data Download	880	44.2
Standby	1.19	Continuous

Battery Life Calculated for Pulsed Conditions

$$\text{Battery Life time (hours)} = \frac{\text{Battery Nominal Capacity (mAh)}}{\text{Total Power Required to Operate for 1 yr (mA)}}$$

<i>No. of D/L</i>	<i>Years of life</i>
0	4.8
1	4.1
2	3.5
3	3.1
4	2.7
5	2.5



Power Failures

Conclusion

	+25°C	-16°C
Life of Data-Recorder Tag (@ 4 data downloads)	21301.77 hrs 2.4 years	21255.64 hrs 2.4 years

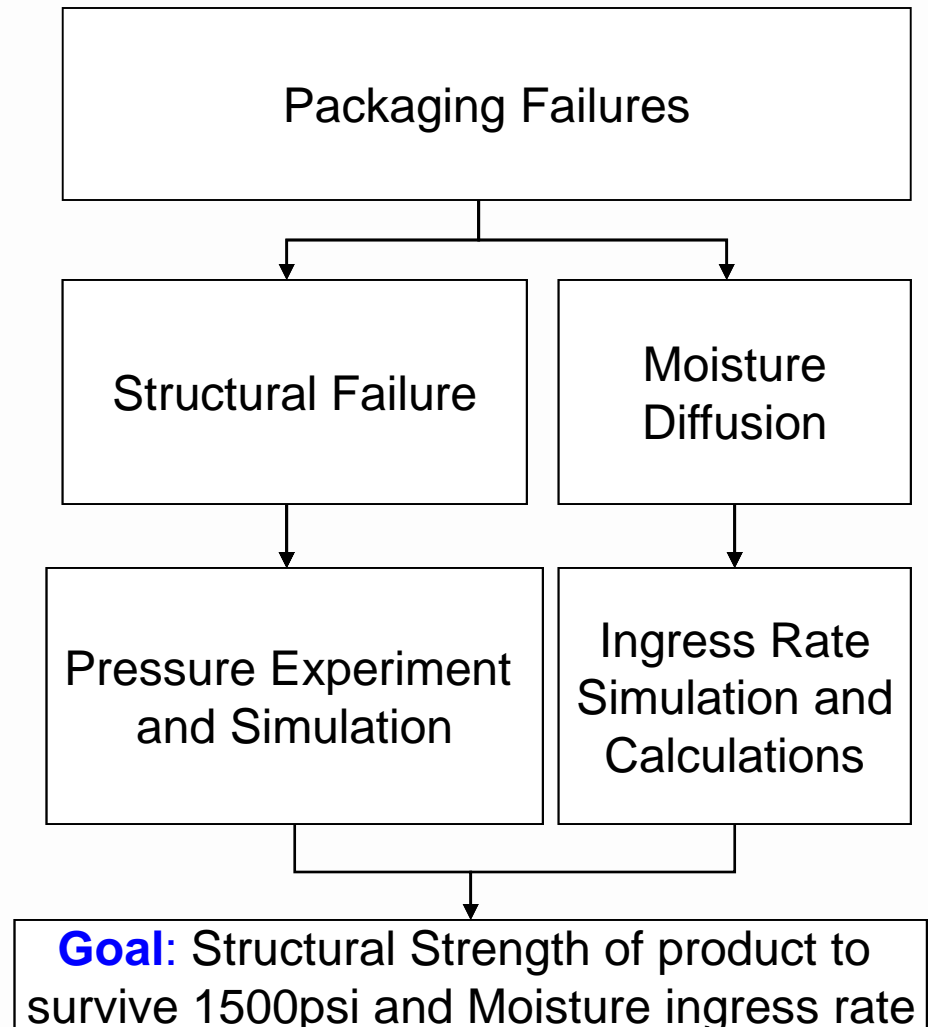
- Life of a Data-Recorder tag is > 2 years
- Battery life is approximately same at +25°C and -16°C
- Power failures are not due to operation in extreme temperature conditions
- Rapid Discharge due to low resistance is explored further in packaging failures

Experiments to Investigate Packaging Failures

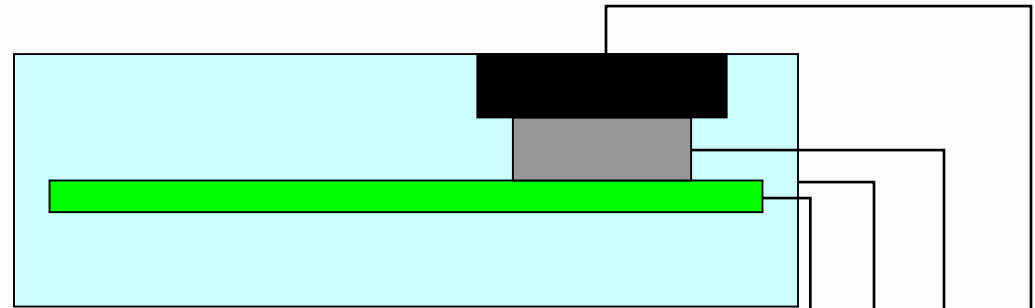
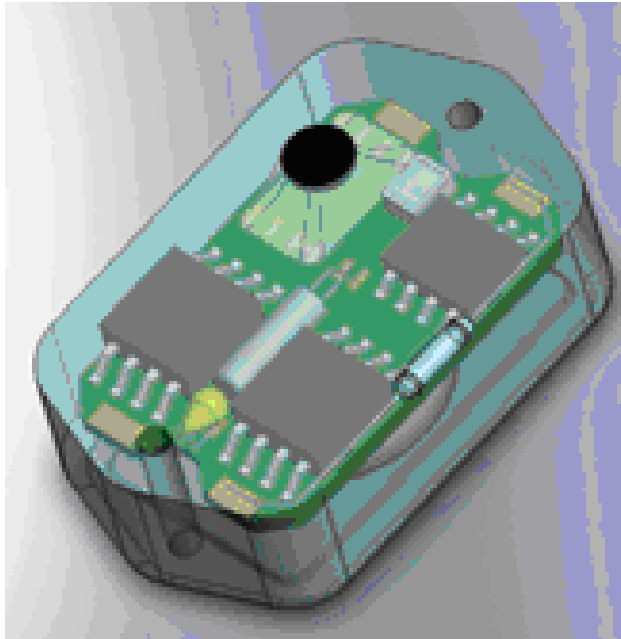
Objective:

To determine

- Yield strength of packaging for 1500 psi rating
- Moisture ingress rate



Plastic Encapsulated Electronics



Soft black polyurethane cap

Pressure sensor die

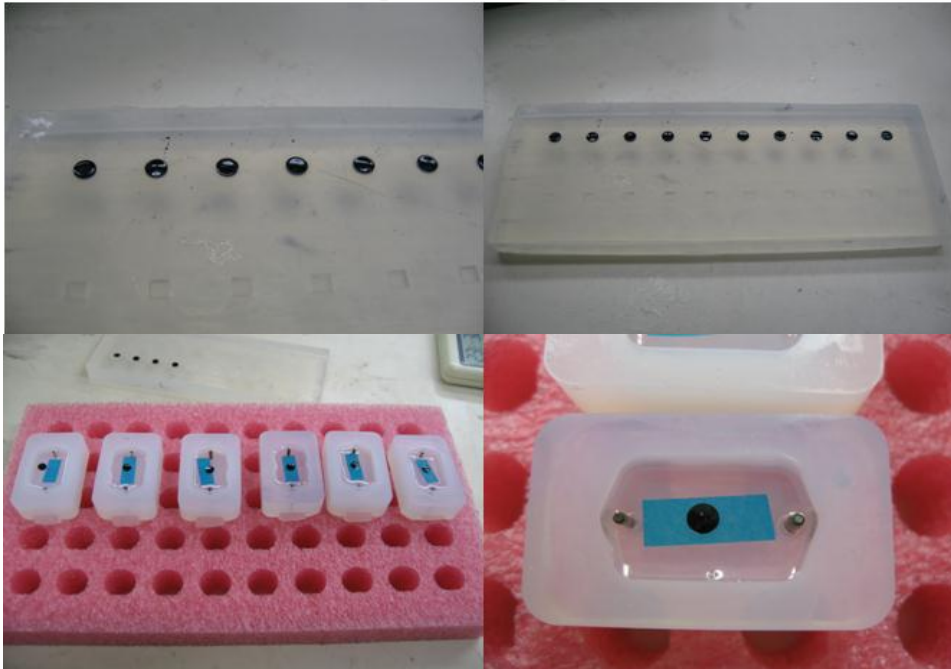
Printed circuit board

Hard clear polyurethane body

Pressure Experiments

Preparations

Sample Preparation



Silicone Moulds



Moisture Test Strip

Test Equipment



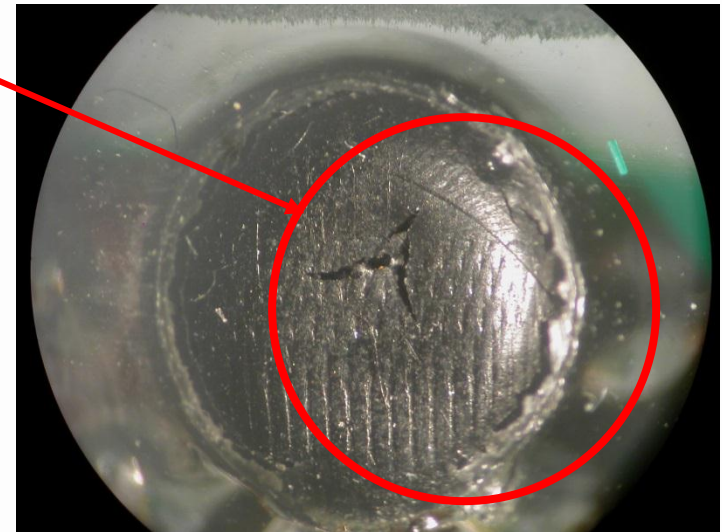
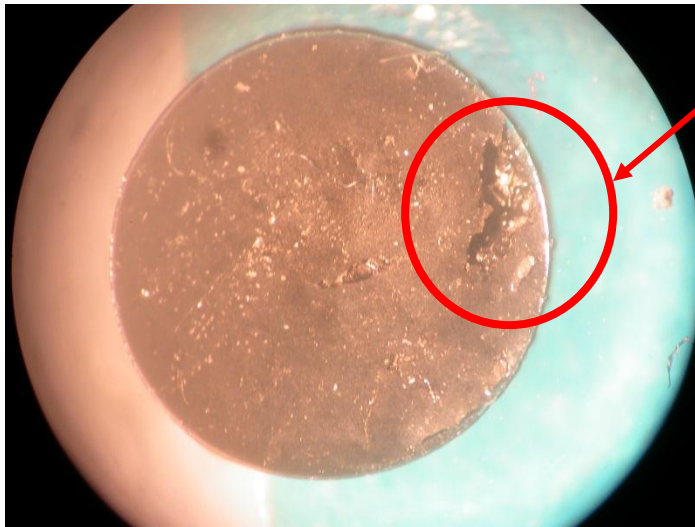
Hydraulic Pressure Vessel

Pressure Experiment

Results

Applied Pressure	Observation
1420psi (1000M)	no damage noticed
2800psi (1975M)	Cracks on black polyurethane cap

Micro cracks @ 2800 psi

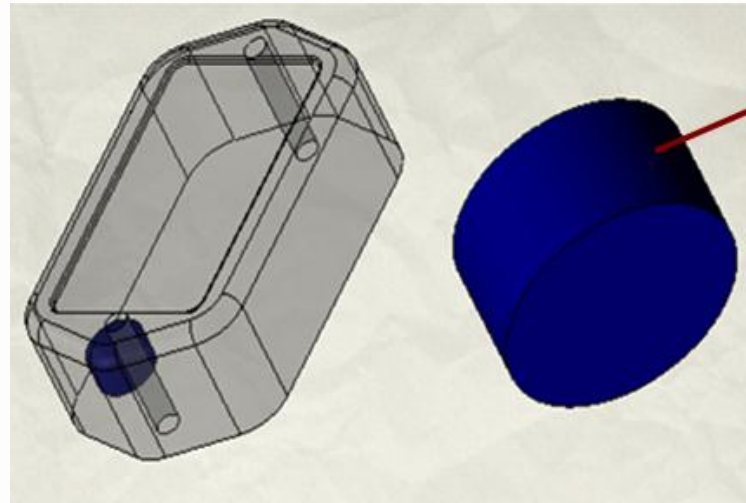


Material Modeling in FEA

- Black polyurethane cap is defined as non-linear visco-elastic material
- Relationship between stress and strain is non-linear
- Non-linearity is caused by material behaviour, large displacements, other
- Non-linear static analysis is conducted to understand creep behaviour of the material

Pressure Simulation

Model



Diameter: 4 mm
Thickness: 2 mm

Material Properties

		Soft Polyurethane (Black)	Hard Polyurethane (Clear)
Elastic Modulus	(N/m ²)	9E06	300E07
Poisson's Ratio		0.49	0.39
Tensile Strength	(N/m ²)	6.89E05	1.99E07
Yield Strength	(N/m ²)	9E06	300E07
CTE (/Kelvin)		0.00067	0.00063
Thermal Conductivity	(W/(m.K))	0.14	0.189
Specific Heat	J/(kg.K)	1	1

FEA Model

Boundary Conditions

Face 2

Translation: $x,y,z = 0,0,0$

Rotation: $x,y,z = 0,0,0$

Face 1

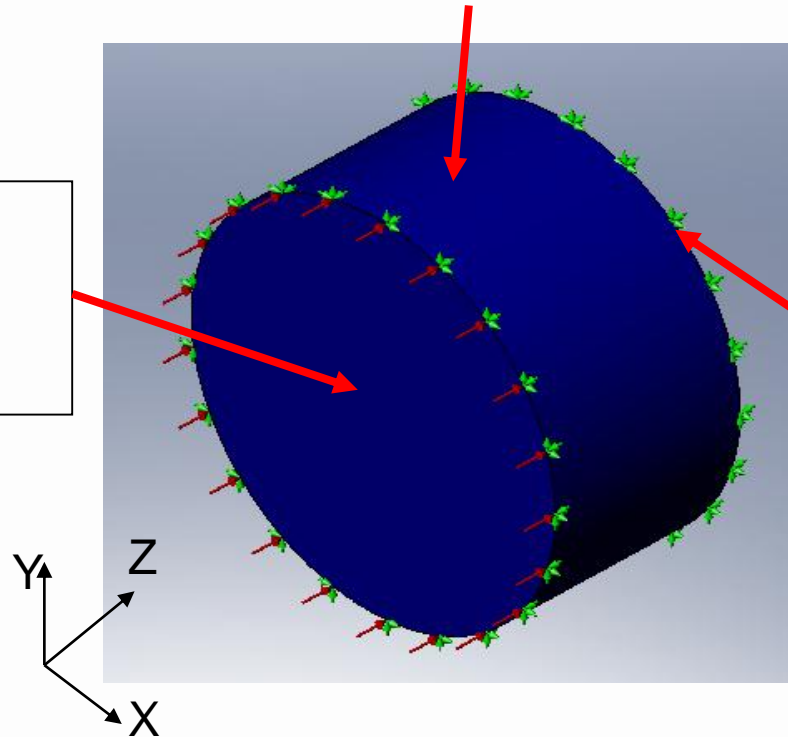
Translation: $x,y,z = 0,0,1$

Rotation: $x,y,z = 0,0,0$

Face 3

Translation: $x,y,z = 0,0,0$

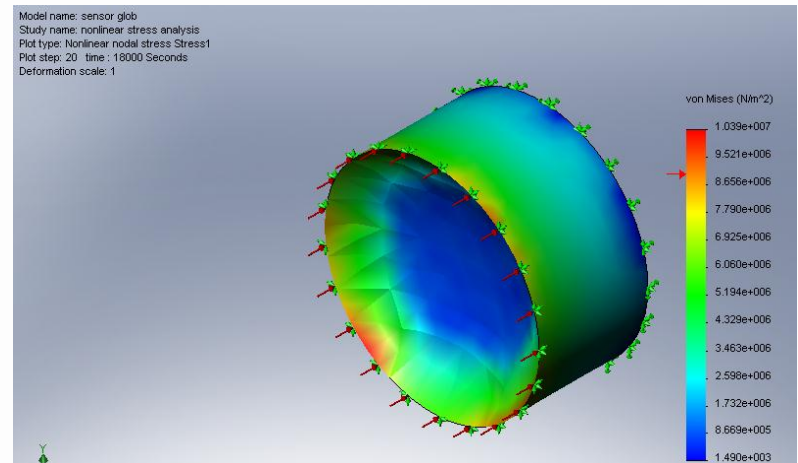
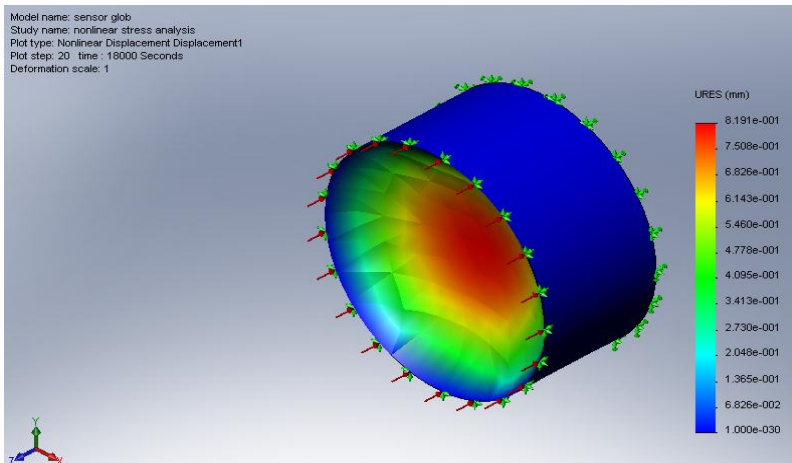
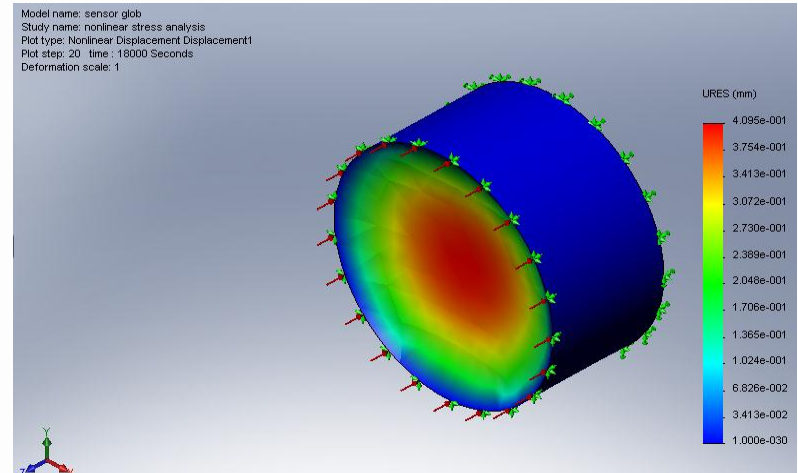
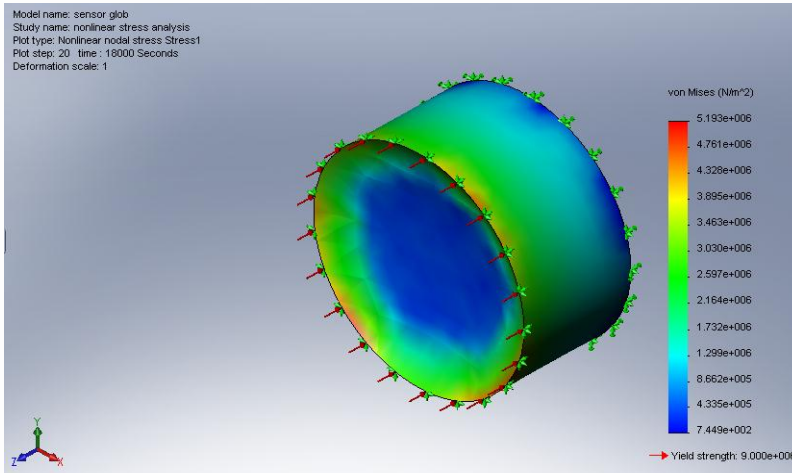
Rotation: $x,y,z = 0,0,0$



FEA Results – Creep Analysis

Stress

Displacement



1420 psi

2800 psi

FEA Simulation

Results

	Creep Analysis (5 hrs)	
	1420psi	2800psi
Von Mises Maximum Stress (N/m ²)	5.19E06	1.039E07
Displacement (mm)	- 0.409	- 0.819

- Stresses exceed yield strength (9E06 N/m²) only when 2800 psi pressure is applied for 5 hours
- FEA simulation results match physical pressure experiment observations

Packaging Failure

Conclusion

(Structural Strength)

- From the animal behaviour as observed through recorded data and published studies, it is not normal for any animal to dive to such depths (2800psi/1975M) and stay there for more than 5-9 minutes
- The packaging design of the data-recorder tag is good for 1500 psi pressure rating

Packaging Failure

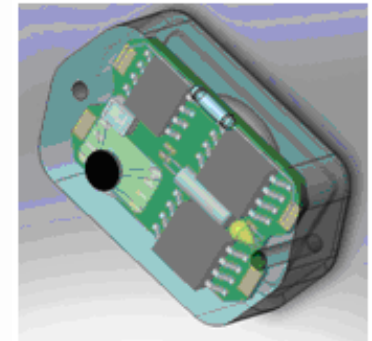
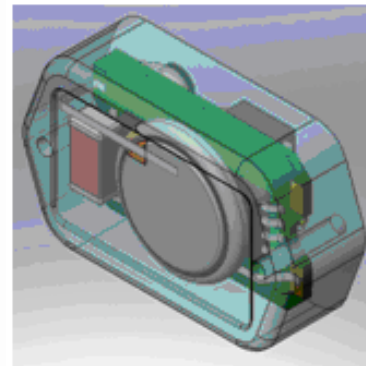
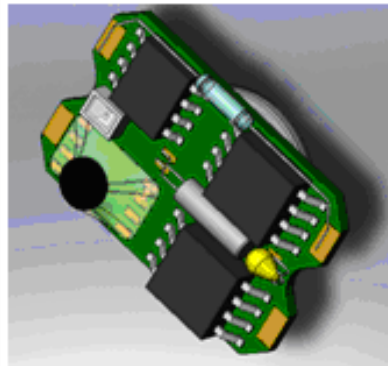
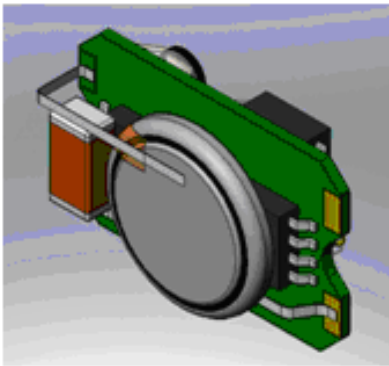
Moisture Diffusion

- Over a period of time moisture diffuses through body material and can reach electronics
- Moisture, if present between two nodes of any component, act as an additional resistance causing low resistance thus resulting in rapid discharge of battery
- Moisture can also completely short circuit any component on the circuit board

Packaging Failures

Water Penetration

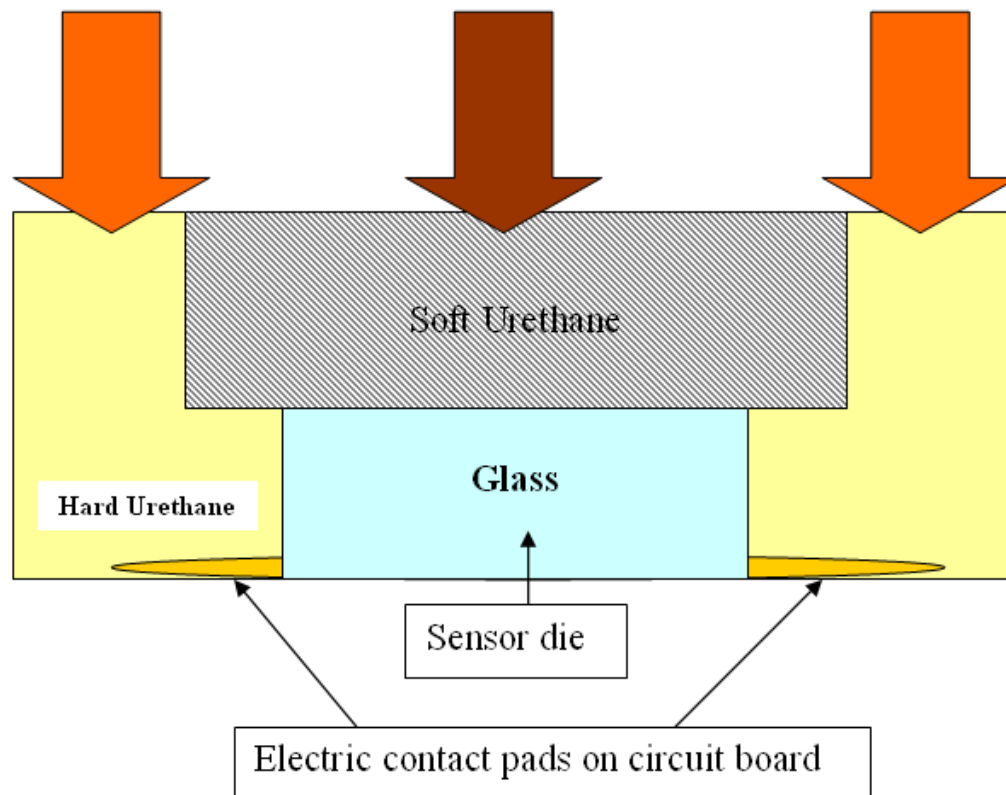
- Penetration of water to electrical circuit
 - Through cracks in plastic encapsulation body
 - Through material by diffusion



Packaging Failure

Moisture Diffusion

Moisture diffusion through material



Diffusion Ingress Rate

$$t_{99\%} = \frac{0.45 h^2}{D}$$

Where,

$T_{99\%}$ = time to approach 99% saturation

h = height or the thickness of the specimen

D = diffusion coefficient

- Material datasheet provided by manufacturer provides the values for M_t/M_∞ obtained experimentally through weight gain experiment (ASTM D570)

$$D = \frac{\pi}{16} \left[\frac{M_t / M_\infty}{\sqrt{t} / h} \right]^2$$

Where,

M_t = total mass of the moisture absorbed at time t

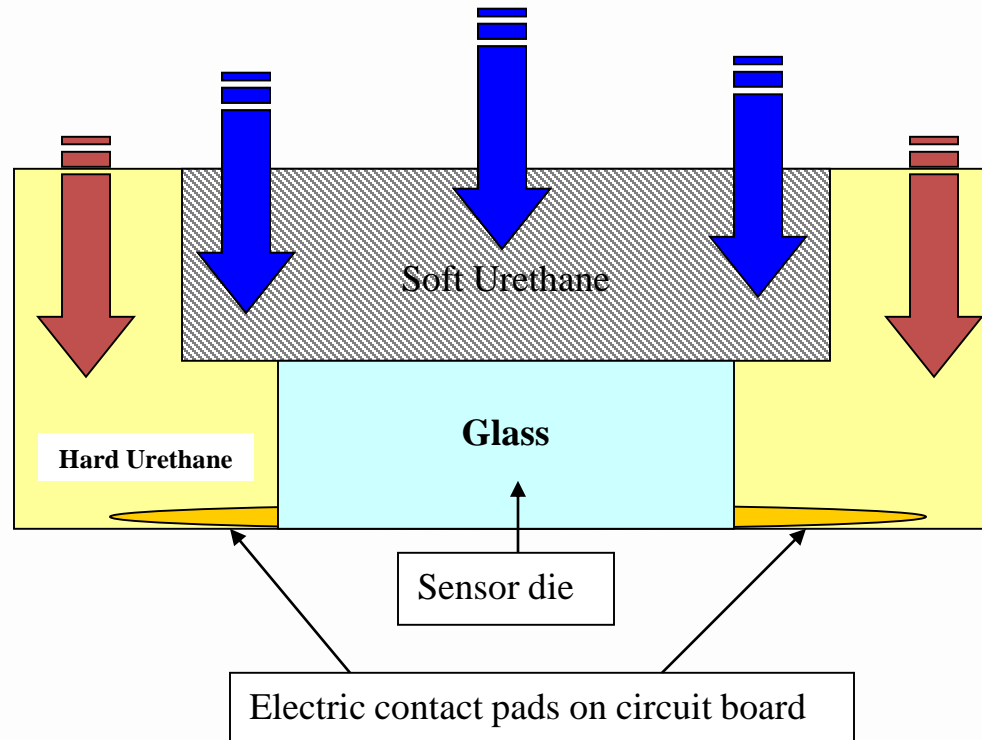
M_∞ = Equilibrium mass of the absorbed substance

h = total sheet thickness (mm)

D = diffusion coefficient (mm^2/hr)

Diffusion Ingress Rate

	Soft Polyurethane	Hard Polyurethane
$t_{99\%}$	178 days (6 months)	2523 days (7 years)



FEA Simulation of Moisture Diffusion

- Process of moisture ingress is similar to transient heat conduction
- Heat Transfer simulation software can be used for moisture diffusion study

Variables Map

Heat Transfer (Temperature, T)		Moisture Diffusion (Moisture Concentration, C)	
ρ , Density	(kg/m ³)	1	
K, Conductivity	W/(m.K)	D, Diffusion Coefficient	(mm ² /hr)
C_p , Specific Heat	J/(kg.K)	1	

FEA Model for Moisture Diffusion

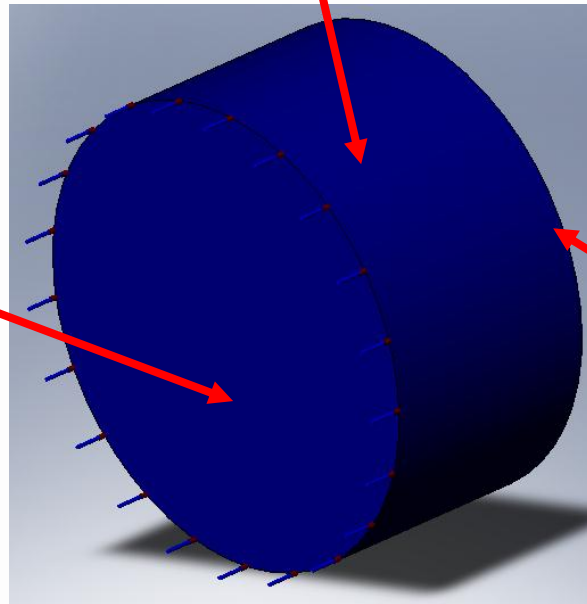
Boundary Conditions

Face 2

Moisture Concentration: $x,y,z = 0,0,0$

Face 1

Moisture Concentration: $x,y,z = 1,1,1$



Face 3

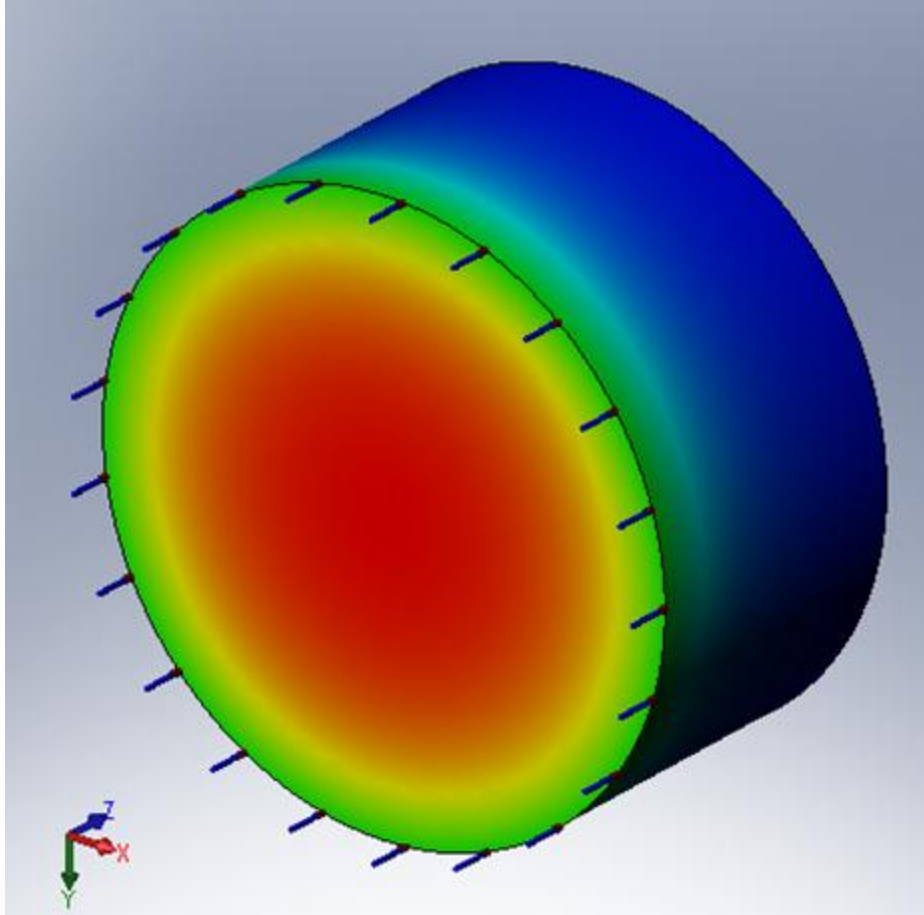
Moisture concentration: $x,y,z = 0,0,0$

Where;

$C = 0$ for complete dryness

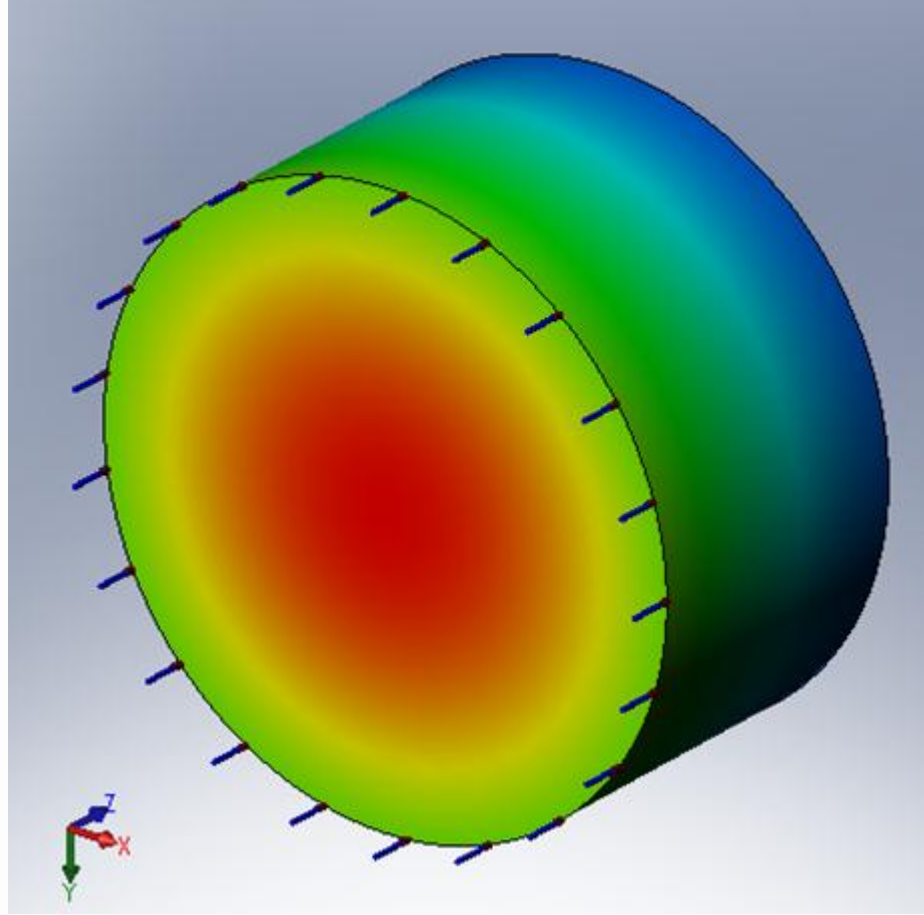
$C = 1$ for saturated wetness

Model name: sensor glob
Study name: moist 2
Plot type: Thermal Thermal1
Time step: 1 time : 155000 Seconds



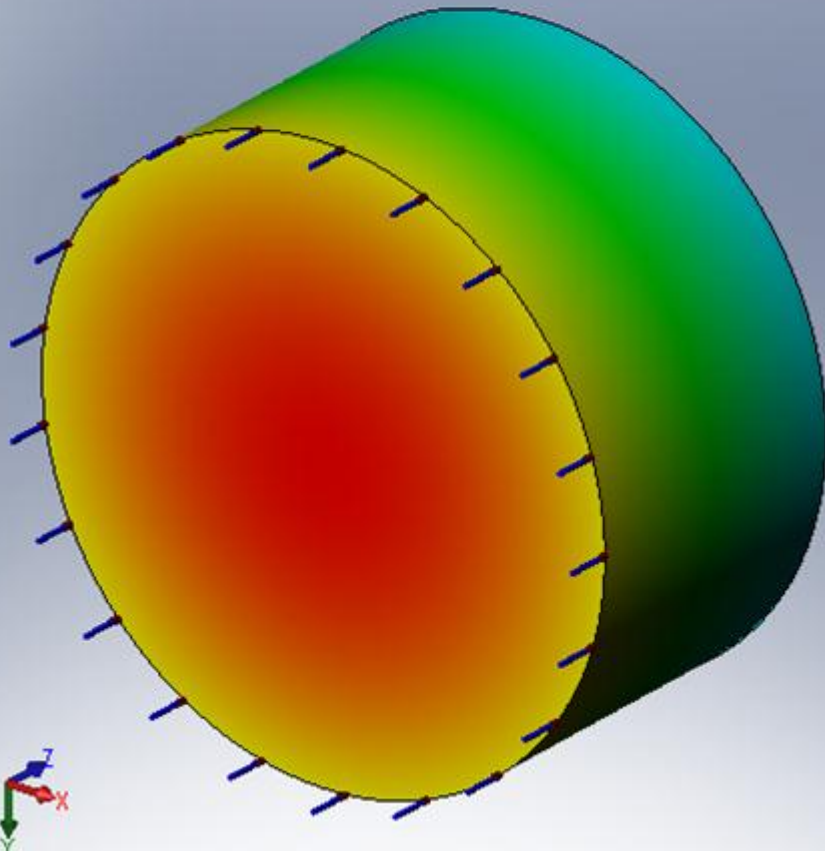
1.8 days

Model name: sensor glob
Study name: moist 2
Plot type: Thermal Thermal1
Time step: 5 time : 775000 Seconds



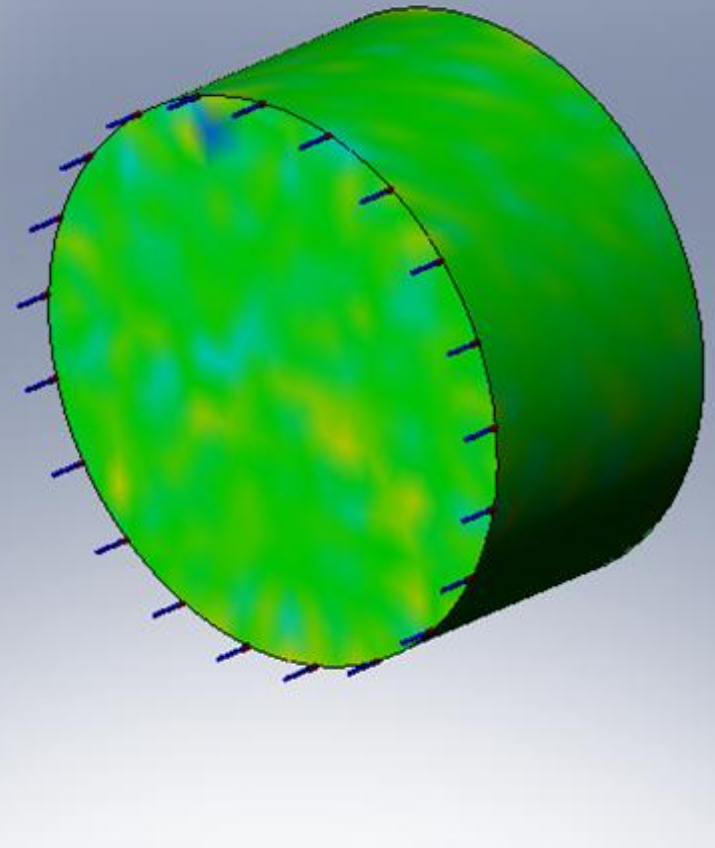
10 days

Model name: sensor glob
Study name: moist 2
Plot type: Thermal Thermal1
Time step: 20 time : 3.1e+006 Seconds



35 days

Model name: sensor glob
Study name: Moisture Diffusion
Plot type: Thermal Thermal2
Time step: 31 time : 1.60164e+007 Seconds



185 days

Packaging Failure **Moisture Diffusion Results**

- It takes approximately 6 months for soft polyurethane to saturate 99% with moisture, whereas approximately 7 years for hard polyurethane.
- Moisture to reach interconnect of pressure sensor which is below the pressure sensor die surface should take more time
- FEA simulation and calculated values match closely

Moisture Ingress Rate (Soft Black Polyurethane Cap)	
Calculated	178 days
FEA	185 days

Conclusions

- Failures are in early life of product, “**Infant Mortality**”, thus Quality Control issue
- Structural strength of tag is good for 1500 psi depth rating
- “Power Failures” are due to presence of moisture
- Moisture breaching plastic body of tag by diffusing through soft polyurethane cap is causing low resistance across component(s) resulting in power failures and/or component failures

Q & A